FAUSKE & ASSOCIATES, LLC

WORLD LEADER IN NUCLEAR AND CHEMICAL PROCESS SAFETY

FAI/09-130-NP

Technical Basis for Gas Transport to the Pump Suction

Submitted To:

PWR Owners Group

(Non-Proprietary Version)

December, 2010

16W070 83RD STREET • BURR RIDGE, ILLINOIS 60527
(877) FAUSKE1 OR (630) 323-8750 • FAX: (630) 986-5481 • E-MAIL: INFO@FAUSKE.COM

Westinghouse Non-Proprietary Class 3

LEGAL NOTICE

This report was prepared as an account of work performed by Fauske & Associates, LLC. Neither Fauske & Associates, LLC, nor any person acting on its behalf:

A. Makes any warranty or representation, express or implied including the warranties of fitness for a particular purpose or merchantability, with respect to the accuracy, completeness, or usefulness of the information contained in this report, or that the use of any information, apparatus, method, or process disclosed in this report may not infringe privately owned rights, or

B. Assumed any liabilities with respect to the use of, or for damages resulting from the use of, any information, apparatus, method, or process disclosed in this report.

COPYRIGHT NOTICE

DISTRIBUTION NOTICE

This report was prepared for the PWR Owners Group. This Distribution Notice is intended to establish guidance for access to this information. This report (including proprietary and non-proprietary versions) is not to be provided to any individual or organization outside of the PWR Owners Group program participants without prior written approval of the PWR Owners Group Program Management Office. However, prior written approval is not required for program participants to provide copies of Class 3 Non-Proprietary reports to third parties that are supporting implementation at their plant, and for submittals to the NRC.

Westinghouse Non-Proprietary Class 3

FAUSKE & ASSOCIATES, INC.

CALCULATION NOTE COVER SHEET

SECTION TO BE COMPLETED BY AUTHOR(S):

Calc-Note Number FAI/09-130 Revision Number 0

Title Technical Basis for Gas Transport to the Pump Suction

Project Develop a Sufficient Criterion to Ensure No Slug Flow to the Pump Suction

Project Number or Shop Order W-PWROG-09-130

Purpose: The purpose of this report is to develop a technical basis and a criterion for the conditions that are sufficient to prevent significant volumes that are formed in the piping high points from being transmitted to the pump suction location as gas slugs.

Summary: A technical basis has been formulated to describe the transition from a separated gas over water flow pattern in the piping high point to bubbly flow in the downcomer through the formation of a kinematic shock. This lead to a conservative criterion to describe the conditions that are sufficient to form this shock. Specifically, the volume of the longest downcomer segment between the piping high point and the pump(s) should be equal to, or greater than, the volume of the gas in the piping high points.

References of Resulting reports, Letters, or Memoranda (Optional)

Author(s): Name (Print or Type)	Signature	Completion Date
Robert E. Henry	Robert E. Henry	December 21, 2010

SECTION TO BE COMPLETED BY VERIFIER(S):

Verifier(s): Name (Print or Type)	Signature	Completion Date
Basar Ozar		December 21, 2010

Method of Verification: Design Review _____, Independent Review or Alternate Calculations X, Testing _____

Other (specify) _____

SECTION TO BE COMPLETED BY MANAGER:

Responsible Manager: Name (Print or Type)	Signature	Approval Date
Robert E. Henry	Robert E. Henry	December 21, 2010

CALC NOTE NUMBER FAI/09-130 **PAGE** 2

CALCULATION NOTE METHODOLOGY CHECKLIST

CHECKLIST TO BE COMPLETED BY AUTHOR(S) **(CIRCLE APPROPRIATE RESPONSE)**

1.	Is the subject and/or the purpose of the design analysis clearly stated?	(YES)	NO	
2.	Are the required inputs and their sources provided?	(YES)	NO	N/A
3.	Are the assumptions clearly identified and justified?	(YES)	NO	N/A
4.	Are the methods and units clearly identified?	(YES)	NO	N/A
5.	Have the limits of applicability been identified? (Is the analysis for a 3 or 4 loop plant or for a single application.)	(YES)	NO	N/A
6.	Are the results of literature searches, if conducted, or other background data provided?	(YES)	NO	N/A
7.	Are all the pages sequentially numbered and identified by the calculation note number?	(YES)	NO	
8.	Is the project or shop order clearly identified?	(YES)	NO	
9.	Has the required computer calculation information been provided?	YES	NO	(N/A)
10.	Were the computer codes used under configuration control?	YES	NO	(N/A)
11.	Was the computer code(s) used applicable for modeling the physical and/or computational problems identified? (i.e., Is the correct computer code being used for the intended purpose.)	YES	NO	(N/A)
12.	Are the results and conclusions clearly stated?	(YES)	NO	
13.	Are Open Items properly identified	YES	NO	(N/A)
14.	Were approved Design Control practices followed without exception? (Approved Design Control practices refers to guidance documents within Nuclear Services that state how the work is to be performed, such as how to perform a LOCA analysis.)	YES	NO	(N/A)
15.	Have all related contract requirements been met?	(YES)	NO	N/A

NOTE: If **NO** to any of the above, Page Number containing justification _____

PWR Owners Group
Member Participation* for Project / Task PA-SEE-0685, Rev. 1

Utility Member	Plant Site(s)	Participant	
		Yes	No
AmerenUE	Callaway (W)	X	
American Electric Power	D.C. Cook 1&2 (W)	X	
Arizona Public Service	Palo Verde Unit 1, 2, & 3 (CE)	X	
Constellation Energy Group	Calvert Cliffs 1 & 2 (CE)	X	
Constellation Energy Group	Ginna (W)	X	
Dominion Connecticut	Millstone 2 (CE)	X	
Dominion Connecticut	Millstone 3 (W)	X	
Dominion Kewaunee	Kewaunee (W)	X	
Dominion VA	North Anna 1 & 2, Surry 1 & 2 (W)	X	
Duke Energy	Catawba 1 & 2, McGuire 1 & 2 (W), Oconee 1, 2, 3 (B&W)	X	
Entergy	Palisades (CE)	X	
Entergy Nuclear Northeast	Indian Point 2 & 3 (W)	X	
Entergy Operations South	Arkansas 2, Waterford 3 (CE), Arkansas 1 (B&W)	X	
Exelon Generation Co. LLC	Braidwood 1 & 2, Byron 1 & 2 (W), TMI 1 (B&W)	X	
FirstEnergy Nuclear Operating Co	Beaver Valley 1 & 2 (W), Davis-Besse (B&W)	X	
Florida Power & Light Group	St. Lucie 1 & 2 (CE)	X	
Florida Power & Light Group	Turkey Point 3 & 4, Seabrook (W)	X	
Florida Power & Light Group	Pt. Beach 1&2 (W)	X	
Luminant Power	Comanche Peak 1 & 2 (W)	X	
Omaha Public Power District	Fort Calhoun (CE)	X	
Pacific Gas & Electric	Diablo Canyon 1 & 2 (W)	X	
Progress Energy	Robinson 2, Shearon Harris (W), Crystal River 3 (B&W)	X	
PSEG - Nuclear	Salem 1 & 2 (W)	X	
Southern California Edison	SONGS 2 & 3 (CE)	X	
South Carolina Electric & Gas	V.C. Summer (W)	X	
So. Texas Project Nuclear Operating Co.	South Texas Project 1 & 2 (W)	X	
Southern Nuclear Operating Co.	Farley 1 & 2, Vogtle 1 & 2 (W)	X	
Tennessee Valley Authority	Sequoyah 1 & 2, Watts Bar 1 & 2 (W)	X	
Wolf Creek Nuclear Operating Co.	Wolf Creek (W)	X	
Xcel Energy	Prairie Island 1&2	X	

* **Project participants as of the date the final deliverable was completed. On occasion, additional members will join a project. Please contact the PWR Owners Group Program Management Office to verify participation before sending this document to participants not listed above.**

PWR Owners Group
International Member Participation* for Project / Task PA-SEE-0685, Rev. 1

Utility Member	Plant Site(s)	Participant	
		Yes	No
British Energy	Sizewell B	X	
Electrabel (Belgian Utilities)	Doel 1, 2 & 4, Tihange 1 & 3	X	
Hokkaido	Tomari 1 & 2 (MHI)	X	
Japan Atomic Power Company	Tsuruga 2 (MHI)	X	
Kansai Electric Co., LTD	Mihama 1, 2 & 3, Ohi 1, 2, 3 & 4, Takahama 1, 2, 3 &4 (W & MHI)	X	
Korea Hydro & Nuclear Power Corp.	Kori 1, 2, 3 & 4 ; Yonggwang 1 & 2 (W)	X	
Korea Hydro & Nuclear Power Corp.	Yonggwang 3, 4, 5 & 6 Ulchin 3, 4 , 5 & 6(CE)	X	
Kyushu	Genkai 1, 2, 3 & 4, Sendai 1 & 2 (MHI)	X	
Nuklearna Electrarna KRSKO	Krsko (W)	X	
Axpo AG	Beznau 1 & 2 (W)	X	
Ringhals AB	Ringhals 2, 3 & 4 (W)	X	
Shikoku	Ikata 1, 2 & 3 (MHI)	X	
Spanish Utilities	Asco 1 & 2, Vandellos 2, Almaraz 1 & 2 (W)	X	
Taiwan Power Co.	Maanshan 1 & 2 (W)	X	
Electricite de France	54 Units	X	

* **This is a list of participants in this project as of the date the final deliverable was completed. On occasion, additional members will join a project. Please contact the PWR Owners Group Program Management Office to verify participation before sending documents to participants not listed above.**

TABLE OF CONTENTS

LIST OF FIGURES

LIST OF TABLES

1.0 BACKGROUND

As part of the combined industry response to NRC Generic Letter 2008-01, the industry has assembled a framework for the extent of noncondensable gas that could be transported to the suction of the Emergency Core Cooling System (ECCS) pumps, without affecting the operability of these pumps, during their response to a Loss-Of-Coolant worst case Accident (LOCA). Specifically, this extent of noncondensable gas characterizes an acceptance criteria for determining the operability state for a plant should gas be detected during the surveillance of the pump suction piping.

Table 1 is taken from NEI (2009) and list the extent of noncondensable gas that the industry has considered could be transmitted to specific pump types without challenging the pump operability. Note that these are expressed in terms of an average void fraction over an interval to determine the extent of gas entering an individual pump. Moreover, these are expressed in terms of (1) when the pump is operating near its Best Efficiency Point (BEP) and (2) for conditions that are below and above this operating region. These criteria have been established as conservative representations of experimental data taken for pump operation in the presence of noncondensable gas, as well as various scale experiments, that characterize the nature of the two-phase (noncondensable gas and water) flow processes sufficient to transport gas from the suction piping high point to the pump suction locations. These characterizations are conservative representations of this information and therefore are appropriate to provide the foundation for operability judgments. This report provides the technical basis for the framework described in Table 1, and specifically the foundation for those necessary conditions that ensure the two-phase mixture flow pattern that is transferred to the pump is bubbly flow, i.e. no gas slugs will be transported to the pumps.

Table 1

Allowable Average Non-Condensable Gas Void Fractions

(to preclude pump mechanical damage) (NEI,2009)

	$\% \frac{Q}{Q_{BEP}}$	BWR Typical Pumps	PWR Typical Pumps		
			Single Stage (WDF)	Multi-Stage Stiff Shaft (CA)	Multi-Stage Flexible Shaft (RLIJ, JHF)
Steady State Operation > 20 seconds	40%-120%	2%	2%	2%	2%
Steady State Operation > 20 seconds	< 40% or > 120%	1%	1%	1%	1%
Transient Operation	70%-120%	10% For ≤ 5 sec	5% For ≤ 20 sec	20% For ≤ 20 sec	10% For ≤ 5 sec
Transient Operation	< 70% or > 120%	5% For ≤ 5 sec	5% For ≤ 20 sec	5% For ≤ 20 sec	5% For ≤ 5 sec

Note: As the result of analyses developed herein, the industry and the NRC representatives have agreed that a peak-to-average of 1.7 is a sufficiently conservative characterization of the average void transient to the pump when assuming that the entire gas volume from the high point is transferred to the pump suction over an interval that is equal to, or less than, the value given above for a specific pump.

2.0 SEQUENCE OF EVENTS IN THE NONCONDENSABLE GAS TRANSPORT

Figure 1 is a schematic representation of a generic PWR piping configuration where noncondensable gas could be accumulated in a suction piping high point that is connected to one or more of the ECCS pumps. Generally, PWRs are configured with a piping header that supplies the individual suction flows for the ECCS pumps. In these configurations, noncondensable gas could be accumulated in local piping high points and could be transported toward the pump suction when one or more of the pumps are started.

The maximum ECCS pump suction demand flow would be generated following the receipt of a LOCA signal. With the subsequent pump starts, the accumulated gas would experience the hydrodynamic transient of the flow demanded by the pumps and would be pulled toward the pump suction location. Figure 2 illustrates the sequence of events for the movement of the gas volume as the flow transient evolves and pulls the gas in the direction of the pump suction, through a local high point and a downturned, downstream elbow. Table 2 lists the sequential features of the transient behavior.

Figure 2d depicts some gas remaining in the downstream downturned elbow. This depends on the Froude number of the flow through the pipe. (For gas-liquid internal pipe flows, the Froude Number is typically defined as $U/[g\ D]^{1/2}$ where U is the one-dimensional superficial liquid velocity, g is the acceleration of gravity and D is the pipe inner diameter.) For example, a Froude number greater than 0.3 is required to move from Figure 2b to 2c and if the Froude number is greater than unity, the gas volume in the downturned elbow will be removed by the flow. Such is the case when dynamic venting is utilized to purge gas from the piping.

As itemized in Table 2, once a pump start begins, the total suction demand is imposed on the downcomer and the first response characteristic is to depressurize the gas space somewhat. Table 2 and Figure 2 denote this pressure in the gas region as P_{gi}. A decrease in this gas pressure caused by the bubble expansion, however small, would be acoustically propagated upstream to the water source thereby initiating flow into the suction piping to support the pump demands.

Figure 1: Generic piping configurations of interest.

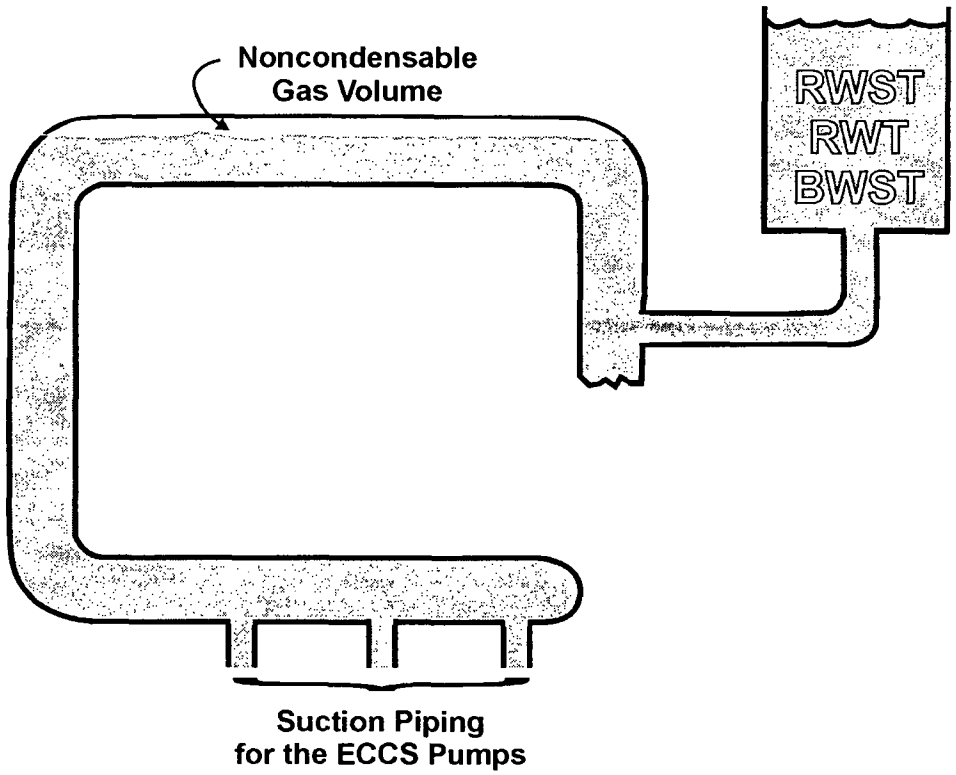

Schematic of a PWR Suction Configuration

20090602-1REH

Figure 2: Transient response of a noncondensable gas volume in the suction piping following initiation of flow.

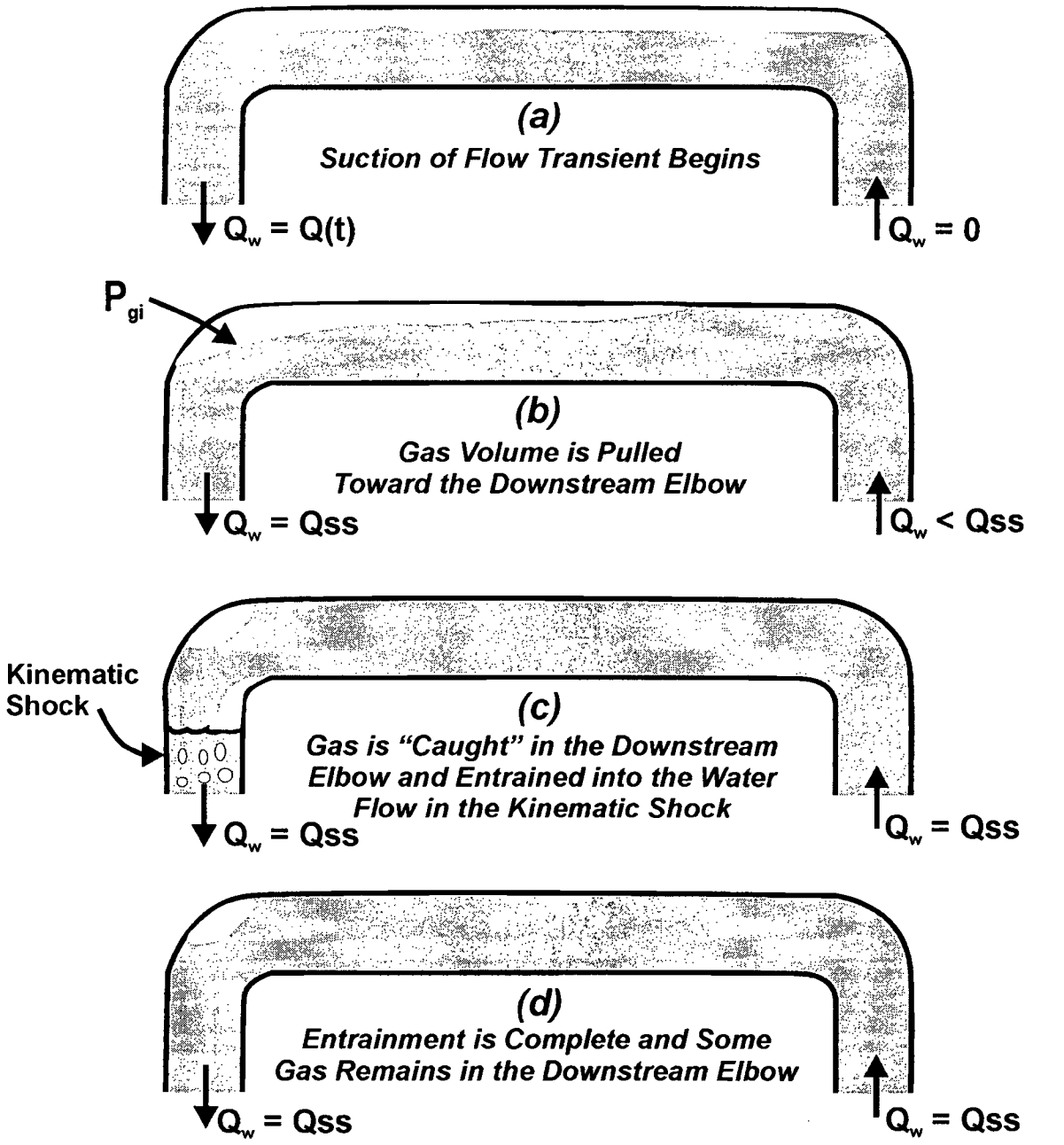

Table 2
Sequence of Events

1.	Pump starts.
2.	Initial flow begins to expand and depressurize the gas space (P_{gi}).
3.	Gas depressurization initiates the supply flow.
4.	A small depressurization (generally about 1 psi) is sufficient for the supply flow to be provided. The extent of the depressurization is configuration specific, but the suction systems are typically designed such that only a small change is needed from the "no flow" condition to supply the steady-state pump flow.
5.	Gas volume is pulled to the downturned downstream elbow until a configuration is developed that can deliver the supply flow.
6.	All gas that is not consistent with the water delivery configuration is pulled into the top of the downcomer.
7.	The gas volume in the top of the downcomer develops a kinematic shock (waterfall) region that experiences gas entrainment, recirculation, disengagement and downward transport of a bubbly flow.

This combination of the pump suction demand in the downcomer and the supply flow from the water source causes the gas to be transported toward the downturned downstream elbow, with the extent of the gas motion being dependent on the water velocity. The gas continues to expand until the upstream volumetric flow rate equals the suction demand on the downcomer. As the water accelerates, the gas volume is pulled into the downstream elbow and the top of the downcomer pipe until a configuration is developed where the upstream volumetric flow rate is sufficient to transport water into the downcomer at a rate that equals the pump demand. (As is discussed later, with Froude numbers in the range of 0.5 to 1, only a small gas bubble could exist in the downturned elbow in the presence of the imposed water volumetric flow rate. For Froude numbers greater than unity, no significant gas volume will remain in the elbow.) For these types of internal flows, the dimensionless Froude number is the ratio of inertial to buoyancy flows and is defined as:

$$N_{Fr} = \frac{U}{\left[\frac{gD\left(\rho_w - \rho_g\right)}{\rho_w}\right]^{1/2}} \approx \frac{U}{\sqrt{gD}} \qquad (1)$$

where D is the pipe internal diameter, g is the gravitational acceleration, ρ_g is the gas density, ρ_w is the water density and U is the one-dimensional, superficial water velocity, i.e. the water volumetric flow rate divided by the pipe cross-sectional flow area.

As a consequence, the transport of gas into the downstream downturned elbow results in pulling much of the accumulated gas into the top of the downcomer as is illustrated in Figure 2(c). For significant initial gas volumes, this gas transport results in a "waterfall" condition in the top of the downcomer, which is a vertically separated flow pattern. Specifically, water pours through, and next to the accumulated gas volume causing entrainment of the gas as the waterfall impinges on the accumulated water pool further down in the downcomer. This transition from a vertically separated flow pattern to a bubbly flow pattern in water pool that is transferred toward the pump is the development of a kinematic shock (Brennen, 2005) at the top of the water column in the downcomer. As noted above, an essential feature of this kinematic shock is that it involves the entrainment of the air by the "waterfall", as the water plunges into the top of the water column. As will be discussed later, the formation of a kinematic shock is dependent on a sufficient volume of the vertical downcomer to accommodate the volume of gas being swept from the high point into the downcomer by the water flow.

The top of the water column can be at a relatively high void fraction region compared to the void fraction that is transported to the pump. In this region, the two-phase flow pattern is one of a plunging water jet entraining air from the gas volume. Some of the gas can remain entrained and transported downward with the remainder of the gas recirculating back to the surface of the kinematic shock and possibly reentering the gas space. It is these details in this kinematic shock that determine the extent of the gas volumetric flow that is transported to the pumps. However, as will be discussed, as long as the downcomer is sufficiently tall to establish the kinematic shock flow pattern for the conditions of interest, the gas void fraction that will be transported to the pumps, will be in a bubbly flow configuration. It is important to note that Table 1 characterizes the extent of the void fraction in the flow that is being transported to the pump suction; not the gas void fraction in the kinematic shock region. Furthermore, in plant applications, the values discussed in Table 1 typically correspond to gas volume accumulations that are a small fraction of the high point piping cross-sectional area. Because most of the gas is

transported into the top of the downcomer, it is the gas volume from the high point that matters, not the void fraction. Specifically, it is important that this gas volume is considerably smaller than the downcomer volume. In particular, when the gas volume is pulled into the downcomer, it is important that a substantial length of water filled piping remains in the downcomer for a kinematic shock to be developed such that the technical basis associated with Table 1 is satisfied. This relationship between the downcomer length and the gas volume is discussed later.

As the air entrainment occurs in the kinematic shock region and the bubbly flow at the bottom of the kinematic shock removes air from the top of the downcomer, the air volume is eroded. Figure 3 shows the manner in which the kinematic shock is formed with the gas volume being eventually consumed by water entrainment. Finally, depending upon the Froude number, only a small gas bubble, if any, would remain in the top of the elbow with the water volumetric flow rate through the high point and the downstream elbow into the downcomer supplying the pump demand flow. Under these final steady-state conditions, the suction flow to the pumps is essentially free of entrained noncondensable gas, i.e. the gas intrusion transient has run its course.

Figure 3

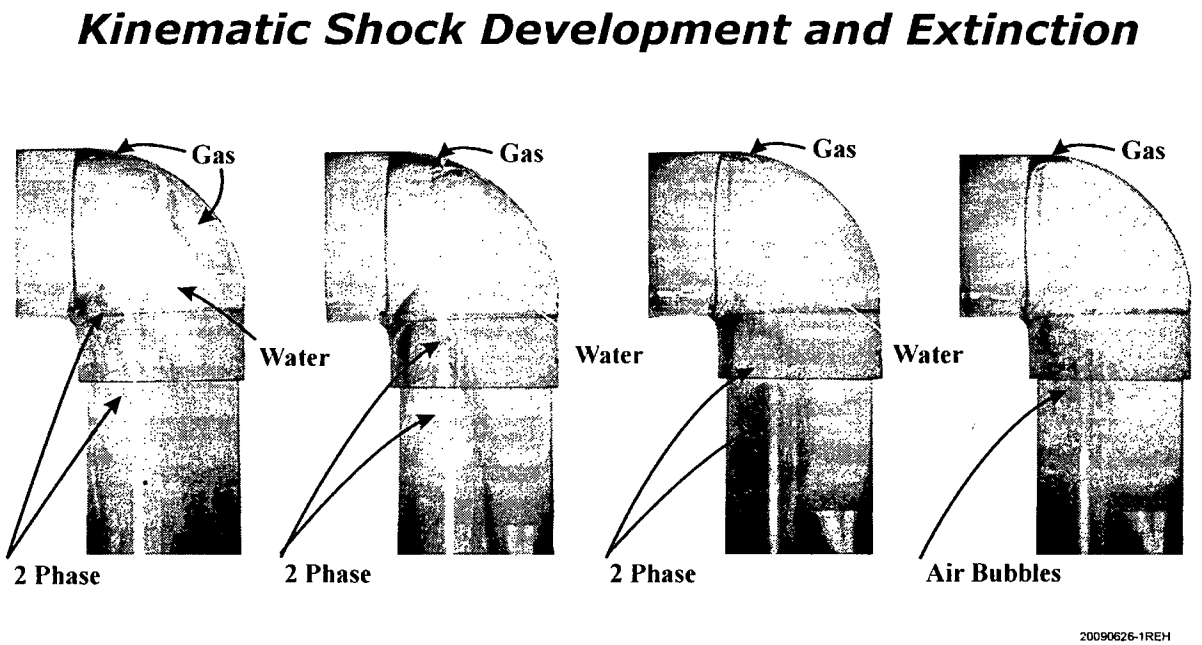
Kinematic Shock Development and Extinction
Gas
Water
2 Phase
Gas
2 Phase
Gas
Water
2 Phase
Gas
Water
Air Bubbles
20090626-1REH

3.0 TECHNICAL BASIS FOR THE INDIVIDUAL FEATURES OF THE GAS VOLUME RESPONSE

3.1 Gas Volume Depressurization

As noted above, the demand flow from the pumps pulls on the gas volume thereby causing it to expand and depressurize. This depressurization propagates upstream to the water source and continues until the volumetric flow rate from the water source equals the pump demand flow rate. The extent of this depressurization can be estimated by quantifying the pressure difference required for fully turbulent flow to supply the demand flow given a pressure difference that can be expressed by

$$\Delta P = f\left(\frac{L}{D}\right)\left(\frac{\rho_w U^2}{2g_c\, 144}\right) \qquad (2)$$

where:

- D is the piping inner diameter (ft),
- f is the Darcy-Weisbach frictional coefficient for fully developed turbulent flow (~ 0.02),
- g_c is the unit conversion constant of 32.2 (lbm/lbf)(ft/sec^2),
- L is the length of the pipe (ft),
- ΔP is the pressure difference (psi) supplying the flow,
- U is the one-dimensional velocity of water through the pipe at the pump demand flow (ft/sec), and
- ρ_w is the density of water in (lb_m/ft^3).

As an example, consider a 24 inch pipe that is 200 feet long with a velocity of 8 ft/sec through the pipe. This corresponds to a Froude number of unity with a volumetric flow rate of over 11,000 gpm. With this length to diameter ratio of 100, the decrease in P_{gi} needed to supply the upstream flow is approximately 1 psi. For a gas volume that had an initial pressure somewhere

between 20 and 50 psia, only a very small expansion would be needed to deliver the upstream (supply) flow at a rate that equals the demand flow rate. As long as the change in pressure is small compared to the initially imposed pressure (usually from the RWST static head) this means that the gas bubble volume remains essentially constant as the flow is initiated and the gas is pulled toward the top of the downcomer. Hence, this can, and should be evaluated for the plant specific design, but if the upstream pressure losses are small compared to the initial pressure there is no significant gas volume change that needs to be considered for the evaluations represented in Table 1.

3.2 Flow Pattern in the Downstream Downturned Elbow

With the suction demand imposed by the pump start, which can be approximated as a linear increase in the volumetric flow rate during the pump run-up interval to the steady-state demand flow rate, the initial response is similar to that shown in Figure 2(b) in which gas is pulled toward the downstream elbow. For those conditions with the Froude number less than approximately 0.35, the gas remains in the piping high point with water flowing beneath the gas volume. This can be conservatively represented as a Froude number of 0.3 leading to conditions under which no gas volume would be pulled into the downcomer and toward the pump. Conversely, above this value, gas entrainment needs to be considered.

For those conditions with Froude numbers greater than 0.35, the gas volume is unable to develop the configuration where the total water flow rate can merely pass beneath the gas bubble. This is due to the extent of flow area required for the increased water flow rate and is related to the characterization of the conditions required for a pipe to run full of water as discussed by Wallis, et al. (1977). In the experimental study conducted by Wallis and co-workers, it was concluded that Froude numbers greater than 0.56 would transport the gas volume out of the downstream end of a horizontal pipe that opened into a large gas space. When considering piping high points, the downturn configuration in the downstream elbow forces gas to accumulate in the downstream elbow with the upstream piping running full of water. In the near vicinity of the elbow, the water, which is flowing at a volumetric flow rate equal to the pump suction flow rate, can accelerate under some small volume of gas bubble as illustrated in

Figure 4. As will be shown, this bubble is relatively small (depending upon the Froude number) and therefore the remaining volume of gas would be pulled into the top of the downcomer and, assuming that the necessary conditions for the required water volume within the downcomer are satisfied, the transported gas volume would form a kinematic shock (see Figure 3). The extent of flow beneath the gas bubble can be estimated by considering that the water flow is initially traveling at velocity U_o, and as illustrated in Figure 4, can be accelerated by an additional pressure decrease due to the decrease in water head as given by:

$$\Delta U \approx \left[g(D - z) \right]^{0.5} \tag{3}$$

where the value of z is defined in Figure 4. Hence, the volumetric flow rate under the gas bubble can be described by the equation:

$$Q_w = A_w \left[U_o + \sqrt{g(D - z)} \right] \tag{4}$$

where A_w is the cross-sectional flow area for the water beneath the gas bubble. With the gas bubble confined in the upper region of the pipe, it will occupy a segment of the cross-sectional area such as that defined in Appendix A to this report. As illustrated in the appendix, to the first order, the cross-sectional area of this bubble can be approximated as having a linear relationship with respect to the ratio of the water height divided by the pipe diameter (z/D). Therefore, the volumetric water flow rate can be represented using a linear representation of the flow area with respect to the dimensionless water height, i.e.

$$Q_w = \left(\frac{z}{D} \right) \frac{\pi D^2}{4} \left[U_o + \sqrt{g(D - z)} \right] \tag{5}$$

As illustrated by this equation, when z = D, there is no gas bubble and when z = 0 there is no water flow rate. The solution for water flow under a gas bubble would exist at the water depth z that maximizes this expression. This maximum would occur at a point where the derivative dQ_w/dz is equal to 0. Differentiating the above equation results in a condition of

Figure 4: Water flow accelerating under a stationary gas bubble.

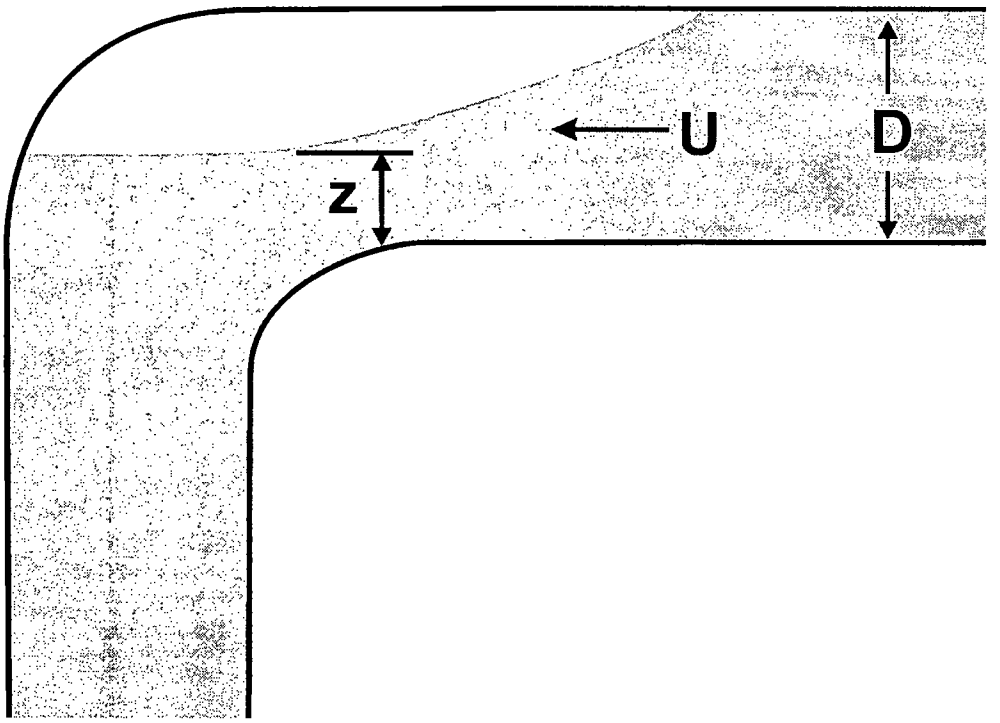

$$\frac{z}{D} - \frac{2}{3}\left[1 + N_{Fr}\sqrt{1 - z/D}\right] = 0 \qquad (6)$$

where N_{Fr} is the Froude number defined by $U_o/\sqrt{gD}$. For a given Froude number, this expression can be solved to provide an estimate of the water depth under the gas bubble. For example, with a Froude number of unity, the dimensionless water depth has a value of 0.89, which for this linear representation of the gas cross-sectional area suggests that a single, stable gas bubble can be formed that occupies 11% of the piping diameter. Reviewing Figure A-2 shows that with the non-linearity of the actual function, and the true value would be closer to 17%. Nonetheless, the assumed functionality is sufficient to demonstrate that a stable gas bubble can be formed with water flowing beneath the surface. However, this stable gas bubble is only of limited depth and only in the downstream elbow, where it is retained by its buoyancy and the imposed water flow rate. Figure 5 shows the calculated dimensionless water depth when the supply flow equals the suction flow rate. As is illustrated in Figures 2 and 3, the remaining gas volume would be transported into the top of the downcomer pipe as part of the response to the pump suction demand.

Figure 3 shows the initial behavior at the top of the downcomer is one of a waterfall that is detached from the inner diameter of the vertical pipe with the depth of this gas volume being determined by the volume of gas that is pulled into the downcomer pipe by the pump suction flow. Figure 3 also shows that once this flow pattern is established, the gas volume is eroded by water entrainment with the erosion rate being dictated by the downward transport of gas bubbles entrained in water. Between the detached and bubble flow regions is a two-phase recirculating region where some of the gas is transported from this mixing zone to the gas volume. As discussed in Section 3.1, this gas volume remains at a constant pressure since any reduction in the intermediate pressure (P_{gi}) would increase the water supply flow to the high point region which would exceed the pump suction demand (Q_w). Hence, the erosion of the gas volume occurs at essentially constant pressure.

It is to be noted that the intent of this analysis is to show that only a very small residual gas bubble would reside in the top of the downturned elbow. The calculations clearly show that

Figure 5: Calculated dimensionless water depth for water flow under a gas bubble.

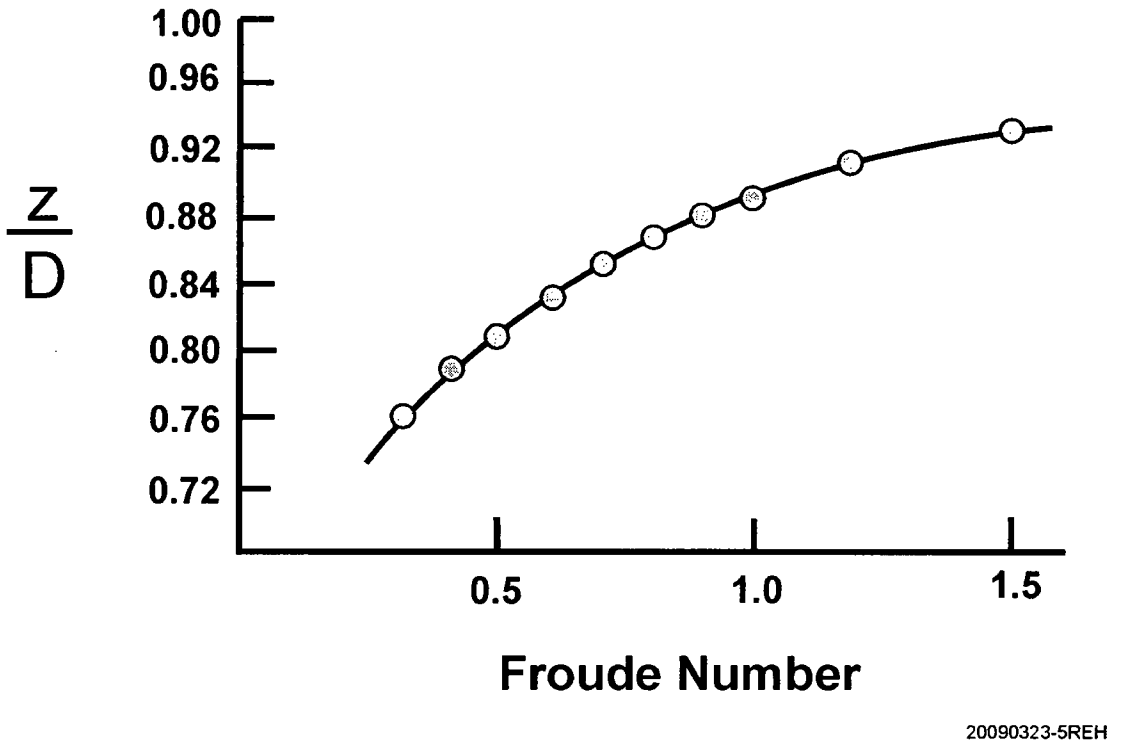

this is true, i.e. for a Froude number of unity, the calculation shows that the depth of the bubble is only 10% of the pipe diameter (water length is 90% of the pipe ID) and the analyses in Appendix A show that this is a void fraction of only 5%. Moreover, since the gas volume has been transported into the downturned elbow and the downcomer, this residual gas void fraction is only in the downturned elbow, i.e. it is a small gas volume. Furthermore, experimental results, like those in Figure 3, demonstrate that a sustained water flow at a Froude number of unity, or above, can entrain the remaining gas volume such that it is eventually consumed.

3.3 Gas Entrainment

Once the kinematic shock is formed, that part of the gas volume that is not consistent with the stable gas bubble at the top of the elbow is eventually entrained as a result of the kinematic shock, i.e. a complicated two-phase flow entrainment processes. This kinematic shock formation and the subsequent entrainment of the gas have been observed in large scale downflow tests, such as those reported by Hammersley et al. (2006). (A summary of these test results is provided in Appendix B.) These tests examined the transport of a completely voided horizontal pipe that was simultaneously opened to a high pressure water source (the containment sump) on one end and a long vertical downcomer on the other. Figure 6 illustrates the essential features of this test configuration. While these represent the extreme conditions of a completely voided pipe, the transient also included all of the phenomena identified in Figure 2, i.e.

- Transport of gas from a high point due to the pump suction flow,
- the formation of a kinematic shock in the top of the downcomer, and
- a measurement (differential pressure) of the two-phase void fraction at the bottom of the downcomer.

These tests were initiated by a simultaneous opening of the two butterfly valves that bounded the completely voided region. This exposed the horizontal gas filled pipe to the upstream water and pressure (P_{CS}) of the simulated containment sump. Within about 3 secs, this pressurized the gas volume from its initial pressure of 5 psig (19.5 psia) to 15 psig (29.5 psia) such that the gas void fraction was reduced to two-thirds of its initial volume, i.e. from 100% to 66%. Pressurization of

Figure 6: Schematic of the test facility reported by Hammersley, et al. (2006).

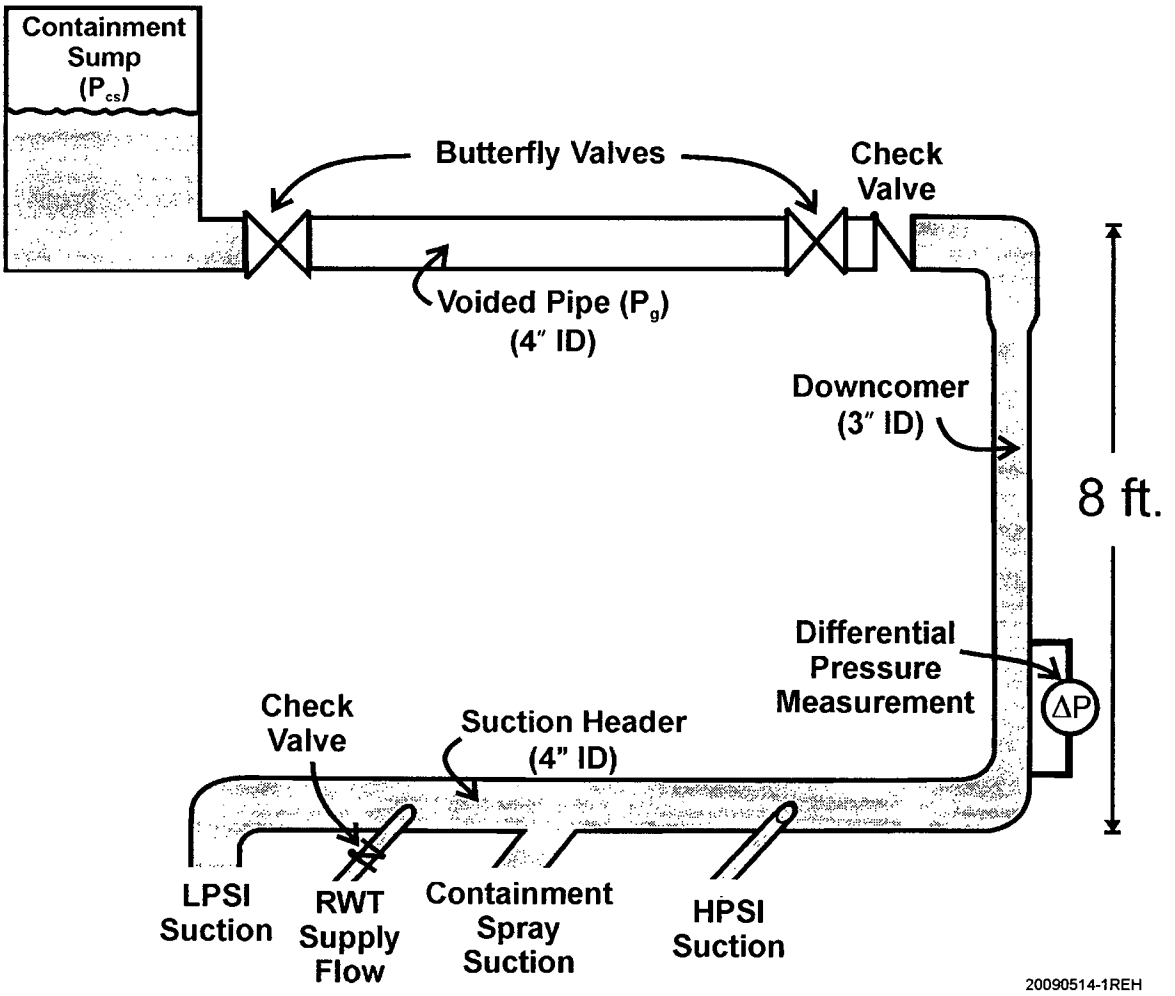

the gas volume caused the downstream check valve to open such that the downcomer and suction header piping was pressurized sufficiently that the RWT check valve closed. From this point on, the flow from the high point location was pulled by the suction flow of the operating pumps of the High Pressure Safety Injection (HPSI) and containment spray systems. (At this stage in the accident response for the Palo Verde reactors, the Low Pressure Safety Injection (LPSI) pumps would be secured.) Transportation of the gas volume into the downstream elbow and the top of the downcomer caused a kinematic shock to be formed which controlled the resulting transport of the gas-water mixture through the downcomer. This integral system experiment provides important insights into the two-phase flow pattern of interest at the bottom of the downcomer.

As the gas volume would be pulled into the downstream elbow and the top of the downcomer, depending on the size of the gas volume, a sufficient gas region could be formed such that the water could detach from part of the vertical downcomer wall and a waterfall could result with the water pouring through the remaining gas volume. Once again it is emphasized that a waterfall would only form for the larger gas volumes since the small volumes would likely be transported as continuous bubbly flow. However, it is essential to appreciate that when a waterfall and a kinematic shock are formed, this is the mechanism to transfer the gas-water flow from a separated flow pattern (annular or slug flow) to a bubbly flow that would then be transported to the pump. Consequently, this flow regime transition serves a very important function in limiting the influence of the gas volume on the pump performance.

This vertically separated flow pattern in the waterfall provides an open space enabling the water to accelerate due to gravity with the velocity increasing according to:

$$U(y) = U_o + \sqrt{2gy} \tag{7}$$

where y is the vertical distance shown in Figure 7. Since the water volumetric flow rate remains constant during the gravitational acceleration, the cross-sectional flow area decreases as the velocity increases.

$$A(y) = Q_w / U(y) \tag{8}$$

Figure 7: Waterfall and gas entrainment by the high velocity jet entering the water.

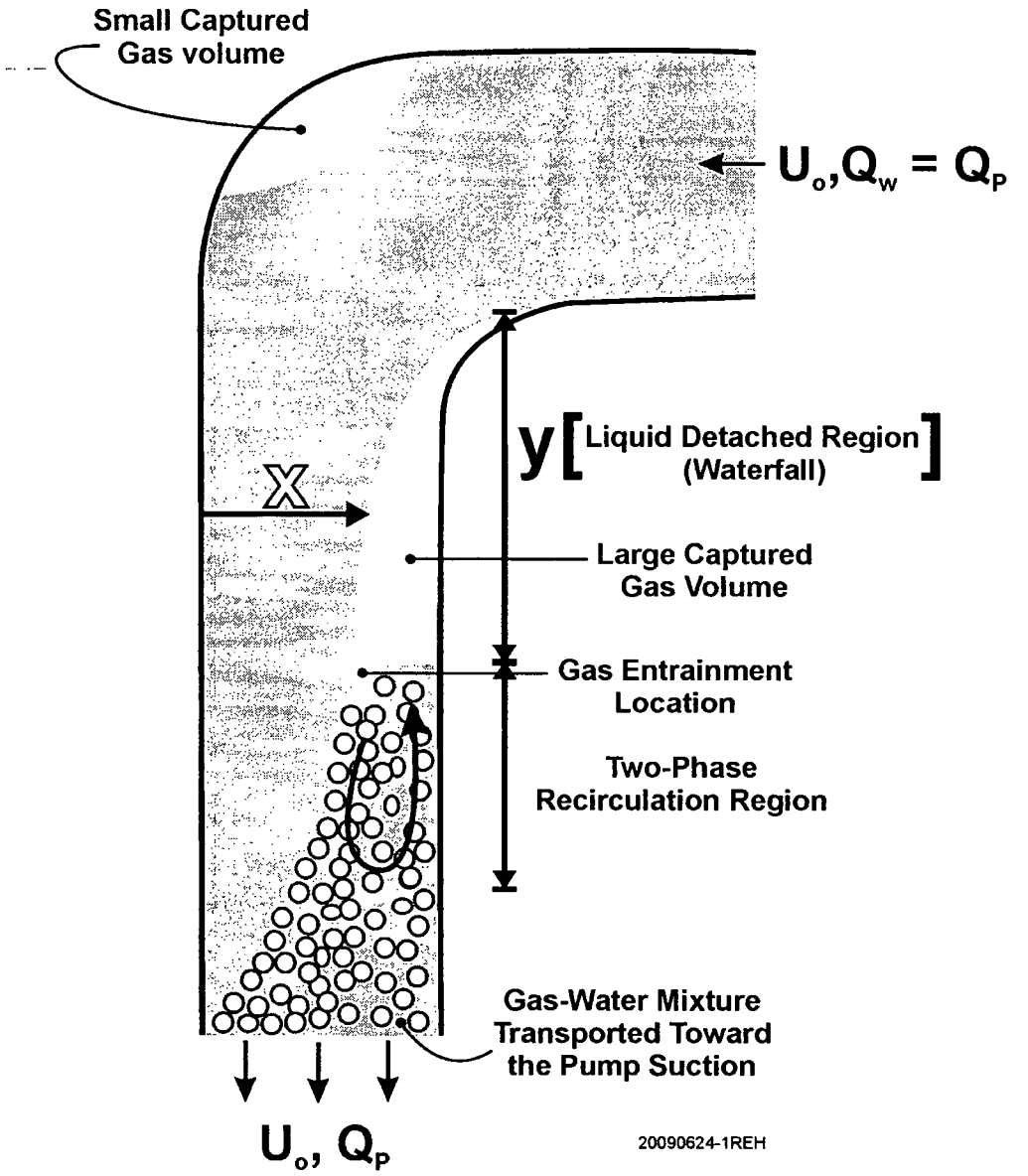

Assuming no entrainment of air as the water descends to the top of the water column in the downcomer (the entrainment zone), a distance of y_1, the waterfall velocity entering this zone can be expressed by:

$$U_1 = U_o + \sqrt{2gy_1} \qquad (9)$$

with the corresponding flow area being equal to the quotient Q_w/U_1.

As this water jet plunges into the upper surface of the downcomer water, gas is entrained as a result of the entry process. Bin (1993) has authored an extensive review article on the numerous studies that have investigated this entrainment mechanism and also documented the correlations that have been constructed to represent the volumetric flow rate of air entrained as a function of the water volumetric flow rate. There are two correlations presented in this review that address the gas volumetric entrainment rate as a function of the water flow rate. These can be expressed in the following ways:

$$\frac{Q_g}{Q_w} = 0.04\, N_{Fr,j}^{0.56} \left(\frac{y_1}{d_o}\right)^{0.4} \qquad (10)$$

$$\frac{Q_g}{Q_w} = 0.09 \left(\frac{y_1}{d_o}\right)^{0.65} \qquad (11)$$

In these equations, the first of which was proposed by Biri (1988) and the second by van de Donk (1981), the terms are defined as:

- d_o is the initial water jet dimension before the water accelerates due to gravity,
- $N_{Fr,j}$ is the jet impact Froude number defined as $U_1/\sqrt{gd_o}$ where U_1 is the water impact velocity,
- Q_g is the volumetric flow rate of the entrained gas and
- Q_w is the water volumetric flow rate.

Both of these correlations where developed from experimental data with circular water jets plunging into a water pool. Considering that the jet impact velocity can be approximated as $U_l = \sqrt{2gy_l}$, the first correlation can be cast in a similar form to that of the second correlation, which is:

$$\frac{Q_g}{Q_w} = 0.049\left(\frac{y_l}{d_o}\right)^{0.68} \tag{12}$$

As shown in Figure 3, because of its greater density, water tends to flow along the outer wall of the downturned elbow and the downcomer pipe, with the gas concentrated along the inner wall. As such, this waterfall configuration is more planar than circular, so this correlation is used to investigate the potential gas entrainment caused as the waterfall plunges into the water filled part of the downcomer. Furthermore, it is noted that the air-water configuration changes from the stratified configuration in the high point to the waterfall in the downcomer, the air and water "pass through" each other in the transient process of transitioning from one flow regime to the other. This is a complicated transition and is expected to cause somewhat more entrainment than is represented by the correlation of jet impingement experimental data. Therefore, this would suggest that the correlation with the larger coefficient is used to maximize the entrainment rate. For assessing the conditions that would prevent a gas slug from penetrating through the downcomer volume, the use of the smaller coefficient is conservative and will be used here.

Through this entrainment mechanism, the captured gas volume is continually eroded, by the entrainment mechanism illustrated in Figure 7, until the gas is completely entrained and transported toward the pump. At the same time, any gas bubble that could exist in the top of the pipe, while limited in size, could remain in this location indefinitely.

In the vertically separated flow pattern associated with the waterfall configuration, the water jet is free to accelerate due to gravity with the velocity increasing as a function of the freefall distance as given by equation (7). As noted above, the velocity increases will be accompanied by a decrease in the cross-sectional flow area such that the volumetric flow rate

remains constant. Since the water tends to remain attached to the far wall, this cross-sectional flow area can be approximated as a linear function of the water thickness (x) illustrated in Figure 7 and can be represented as:

$$A(y) = \frac{\pi}{4} Dx(y) = K_1 \, Dx(y) \tag{13}$$

In this equation, D is the pipe diameter and x is the dimension from the far wall to the air/water interface which is also a function of y. Since the volumetric flow rate remains constant, the value of x as a function of y is given by

$$x(y) = \frac{Q_o}{K_1 DU} = \frac{Q_o}{K_1 D\left[U_o + \sqrt{2gy}\right]} \tag{14}$$

Referring to Figure 7, the volume of water that exists in this acceleration region is bounded by the beginning of the acceleration flow (the bottom of the horizontal pipe) and the location where the water jet plunges into the accumulated water mass at the bottom of the gas void. This water volume is represented by the integral of the water thickness (x) over the length y_1.

$$V_w = \int_o^{y_1} K_1 \, Dx(y) \, dy = \int_o^{y_1} \frac{Q_o}{U_o + \sqrt{2gy}} dy \tag{15}$$

The solution to this integral is:

$$V_w = \int_o^{y_1} \frac{Q_o}{U_o + \sqrt{2gy}} dy = \frac{Q_o}{g} \left[\sqrt{2gy_1} - U_o \ln\left(U_o + \sqrt{2gy_1}\right) + U_o \ln\left(U_o\right)\right] \tag{16}$$

This is not a convenient analytical equation to use for some applications. An approximation to the solution of this integral is given by

$$V_w = (Q_o/U_o)\, y_1 \left(1 + N_{Fr}^{-1} (y_1/D)^{1/2}\right)^{-1} \tag{17}$$

The total volume in this acceleration zone is the sum of the water and gas volumes; hence, the gas volume can be expressed by

$$V_g = A_o y_1 - V_w \tag{18}$$

such that the depth of the kinematic shock region (the length y) can be expressed by:

$$y_1 = \frac{1}{A_o}\left(V_g + V_w\right) \tag{19}$$

Substituting the expression for the water volume into the equation and using a new variable y* that is defined as

$$y^* = y_1^{1/2} \tag{20}$$

results in the cubic equation

$$(y^*)^3 = \alpha_{hp} L_{hp} [N_F (D^{1/2}) + y^*] \tag{21}$$

In this equation, the value of y* that satisfies this equation can be determined by assuming a value (for example zero) for y* in the right hand side of the equation and calculating a new and better estimate for the assumed value. This new estimate can then be inserted on the right hand side and an improved estimate is calculated. Such a process converges rapidly to the solution for this equation, which is the depth of the kinematic shock for the instantaneous gas volume. As illustrated by the above equation, the value of y* is a function of the gas volume and the depth of the kinematic shock region decreases as the gas volume as the gas volume is eroded. Assuming an initial condition that the entire gas volume is swept into the downcomer, which as noted

previously is a function of the Froude number, the maximum depth of the kinematic shock can be calculated from the above equation which also gives the instantaneous gas entrainment rate.

As the falling water jet plunges into the bubbly two-phase mixture at the top of the accumulated water mass in the downcomer, noncondensable gas is entrained by the entry process as illustrated in Figure 8. Through this entrainment mechanism, the captured gas volume is eroded over time and the entrained gas bubbles are swept along with the imposed water volumetric flow rate toward the pump(s). If the equations were solved numerically with the representation of the gas entrainment rate, the new value for the gas volume at each timestep can be used with the equation for the depth of the kinematic shock to evaluate the instantaneous value of the variable y* and thus the variable y. In this way, the time dependent erosion history of the gas volume can be calculated.

As discussed above, for cylindrical jets, the volumetric flow rate for gas entrainment (Q_g) can be related to the flow rate (Q_w) of the plunging water jet using the form:

$$Q_g/Q_w = - K (y/D)^{0.68} \quad (22)$$

where K is an empirical constant with reported values between 0.049 and 0.090 for different experiments (Bin, 1993). (This minus sign occurs since the entrainment describes the removal rate from the gas volume.) In the correlations reviewed by Bin, the diameter in the denominator is the initial diameter of the water jet as it is discharged from a cylindrical nozzle and y is the freefall distance to the water surface. In this application, the interpretation of y is the same, but the diameter of the water jet is taken to be the piping inner diameter. For the geometry of interest, the waterfall configuration that would evolve following the displacement of the gas volume into the downcomer would be anticipated to be more planar than cylindrical. With these differences, it is expected that the lower value of the coefficients are not only more appropriate value, but are conservative with respect to determining whether a gas slug could penetrate to the bottom of the downcomer.

Figure 8: Entrainment mechanism for plunging liquid jets.

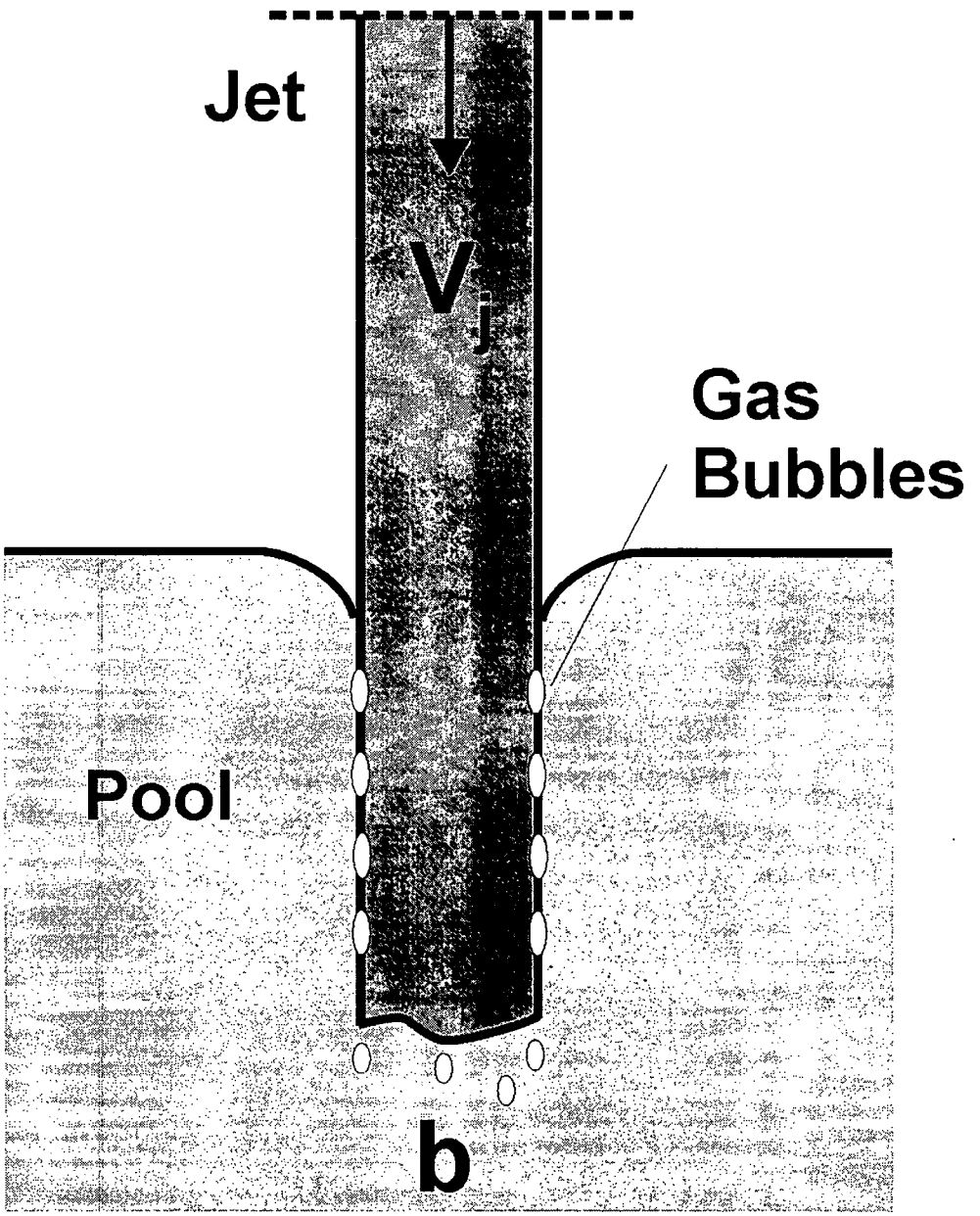

From the functional form of the above entrainment correlation it is observed that the depth of the kinematic shock and the water volumetric flow rate determine the extent of the gas entrainment. In addition, assuming that the entrainment process produces a nearly homogeneous mixture, the ratio of the gas and water volumetric flow rates can also be interpreted in terms of the gas void fraction that would be developed as given by:

$$Q_g/Q_w = \alpha/(1-\alpha) \tag{23}$$

Therefore, once the ratio of the volumetric flow rates is computed by using the depth of the kinematic shock and the piping inner diameter, the homogeneous void fraction corresponding to the gas entrainment rate can be calculated, which represents the value exiting the bottom of the kinematic shock region. As expected, the rate of air entrainment decreases as the depth of the kinematic shock decreases with time as does the entrained void fraction. Consequently, the maximum void fraction α_{max} occurs at the beginning of the transient when the value of y is at its maximum.

The average volumetric gas entrainment flow rate ($Q_{g,avg}$), and therefore the average entrainment void fraction (α_{avg}) can be obtained by integrating the above equation for Q_g with respect to y as it varies from the maximum (y_{max}) to zero and dividing the result by y_{max}. This gives the following expression for the average volumetric gas entrainment flow rate ($Q_{g,avg}$) and the average void fraction:

$$Q_{g,avg}/Q_w = 0.029\,(y_{max}/D)^{0.68} = \alpha_{avg}/(1-\alpha_{avg}) \tag{24}$$

When the depth of the kinematic shock is the greatest, the water generally has a considerably greater velocity as a result of the gravitational acceleration than the one-dimensional velocity in the pipe, and the two-phase mixture at the bottom of the kinematic shock is nearly homogeneous because of the higher velocity. However, below the kinematic shock, the high water velocity associated with the waterfall eventually diffuses to the one-dimensional velocity corresponding to the suction flow rate of the pump(s). With this deceleration, the gas and water can have considerably different velocities due to the influence of buoyancy, i.e. the

decrease in the velocity increases the relative importance of buoyancy. The extent to which this influences the local void fraction at the bottom of the downcomer can be estimated as described in the following paragraph.

From the one-dimensional continuity equations for each of the phases, the ratio between the gas and water one-dimensional velocities is entitled the slip ratio (k_s) and can be expressed in terms of the two-phase mixture mass fraction (quality x_Q), the volume fraction (void fraction α) and the individual phase densities as:

$$k_s = \frac{u_g}{u_w} = \left(\frac{x_Q}{1-x_Q}\right)\left(\frac{1-\alpha}{\alpha}\right)\frac{\rho_w}{\rho_g} \tag{25}$$

As discussed above, in the near vicinity of the kinematic shock, the gas and water velocities are essentially the same (the slip ratio is unity) but begin to diverge from this homogeneous condition (α_H) as the two-phase mixture diffuses to match the pump conditions. This ratio of mass flow rates will remain the same as the flow diffuses and therefore the void fraction at the end of the kinematic shock (α_2) can be related to the flow being transported to the pump as:

$$\frac{1-\alpha_2}{\alpha_2} = \frac{1}{k_p}\left(\frac{1-\alpha_p}{\alpha_p}\right) \tag{26}$$

In this expression, k_p is the slip ratio for the flow where the water velocity has diffused to meet the pump suction conditions. Considering a typical plant situation with the one-dimensional velocity in the suction piping of 7 ft/sec and assuming that the gas bubbles have a relative velocity with respect to the water of approximately a foot per second (as given in Wallis (1969)) for the bubble rise velocity in quiescent water flow, the slip ratio would be 6/7 = 0.86. Substituting this into the above equation for a homogeneous void fraction of 0.23 at the bottom of the kinematic shock, results in a calculated void fraction, considering the slip ratio, of 0.26 at the bottom of the downcomer. As this flow turns into a horizontal leg, the flow can once again be expected to accelerate to essentially a homogeneous condition and possibly even develop a

slip ratio that may be larger than unity. In any case, the horizontal flow would have a lower void fraction; the maximum value of which would be 0.23.

4.0 INFLUENCE OF STATIC HEAD

Many plant suction piping configurations have a significant head difference between the high point location where the gas is accumulated and the location where it would enter the ECCS pumps. Depending on the specific design features, this head difference could result in compression of the gas volume as it is transported to the suction locations for the different pumps. Any such large elevation difference acts to compress the gas and reduce the void fraction entering the pumps. For some designs, this gas volume compression can be significant.

Figure 1 illustrates the point that the high point for PWR systems is typically pressurized by the static head between the water surface in the atmospheric vented borated water storage tanks (RWST, SIRWT, RWT or BWST) and the location of the piping high point(s) of interest. As discussed previously, this initial gas pressure changes only slightly due to the initial suction flow rate developed by the starting of the ECCS pumps. The extent of the gas compression as it flows to the pump suction can be estimated assuming that the gas remains at the water temperature such that the product of the pressure and the gas volume remains constant (isothermal behavior). Considering the gas at the piping high point to be at the pressure P_{gi}, the pressure at a pump due to the static head (P_P) in the units of psia can be estimated by the following expression (considering English units):

$$P_P = P_{gi} + \frac{\rho_w \, g \, z}{g_c \, (144)} \tag{27}$$

where z is the elevation difference (in feet) between the pump suction location and the piping high point. Certainly, this difference is somewhat reduced by the frictional pressure drop between these two locations, which as illustrated previously, is generally a small value compared to the local pressure. Moreover, the static head is also reduced somewhat due to the air that is pulled into the top of the vertical downcomer. However, these are also usually small variations for those configurations where the static head is important. Therefore, this simplified representation of the static head is sufficient to estimate the gas compression without challenging the conservative margins used to represent the entrainment process. With this representation of

the imposed pressure at the pump suction location, the relationship between the volume of gas pulled into the top of the downcomer and the corresponding volume that this gas would represent at the pump suction can be expressed as:

$$\frac{P_P}{P_{gi}} = 1 + \frac{\rho_w \, g \, z}{P_{gi} \, g_c \, (144)} = \frac{V_{gi}}{V_{gP}} = \frac{\alpha_{gi}}{\alpha_P} \tag{28}$$

As also illustrated in this expression, the gas void fraction is correspondingly reduced such that, at the pump suction, this gas void fraction can be calculated by

$$\alpha_P = \left(\frac{P_{gi}}{P_P} \right) \alpha_{gi} \tag{29}$$

Some perspective on the importance of this compression is helpful. A head increase of 1 psi requires a vertical dimension of approximately 2 feet of water and therefore approximately 29 feet of water is required to increase the pressure by 1 atm. If the piping high point is at a pressure near 1 atm, a vertical head of 30 feet would double the imposed pressure and therefore decrease the void fraction by a factor of 2 when it reaches the pump suction. As another example, consider a plant piping configuration where the head difference between the water level in the water storage tank and the piping high point is 45 feet with an additional 30 feet of elevation change to the pump suction. The pressure of the accumulated gas in the high point would be approximately 2.5 atm and, with the additional static head increase of 30 feet to the pump suction, the pressure is further increased to approximately 3.5 atm. Hence, the ratio of these two pressures reduces the gas void fraction to 71% of the value that it had in the piping high point. This demonstrates that the influence of additional compression by the static head is of greater importance for those systems which are not substantially pressurized at the piping high point, i.e. the influence is reduced as the pressure P_{gi} is increased by the imposed static head from the water storage vessel.

5.0 COMPARISON WITH EXPERIMENTS

5.1 Palo Verde Integrated System Scaled Tests

This analytical approach can be compared with the overall observations for the large initial gas volumes experimentally investigated by Hammersley et al. (2006), which are summarized in Appendix B. Specifically, these tests were initiated with a segment of a horizontal pipe that was completely voided between two isolation valves. With the simultaneous opening of these two butterfly valves, the large gas volume was forced into the top of the downcomer pipe, a kinematic shock was formed and transitioned the separated flow pattern into a bubbly flow pattern. This two-phase flow pattern was transmitted out of the bottom of the downcomer and into the horizontal pump suction header. Equally important, these tests included a measurement of the void fraction at the bottom of the downcomer through a differential pressure measurement (see Figure 6), which was dominated by the static head (density head) of the mixture. Figure 9 shows the measured void fraction history in the bottom of the downcomer for Test PVA21, which for this test had a maximum value of about 0.13. (As is noted from the continuity evaluations in Appendix B, at the imposed Froude number of 0.6, most of the test observed that some of the gas remained in the high point piping. This has some bearing on the maximum void fraction in an individual test.) This measured value is of particular interest because, if separated flow patterns of either slug or annular flow could be transmitted to the bottom of the downcomer, the measured static head for the mixture would be zero. (The static head of all vertically separated flow configurations, such as annular or slug flow, is essentially zero.) If any such separated flow conditions were to exist, the void fraction measurement would show a value of unity, which it does not. *Hence, the most important observation from these tests is that, as a result of the kinematic shock, the two-phase flow regime is bubbly flow, not slug flow.* These tests provide the most extreme conditions to enable the transmittal of a gas slug to the bottom of the downcomer, i.e. the tests were initiated with (a) the high point completely voided, (b) a sufficient Froude number to pull the gas into the top of the downcomer and (c) a downward velocity that is sufficient to entrain the gas thereby pulling it through the downcomer pipe to the suction header. As summarized in Appendix B, repeated tests for these conditions

Figure 9: Void fraction history at the bottom of the downcomer.

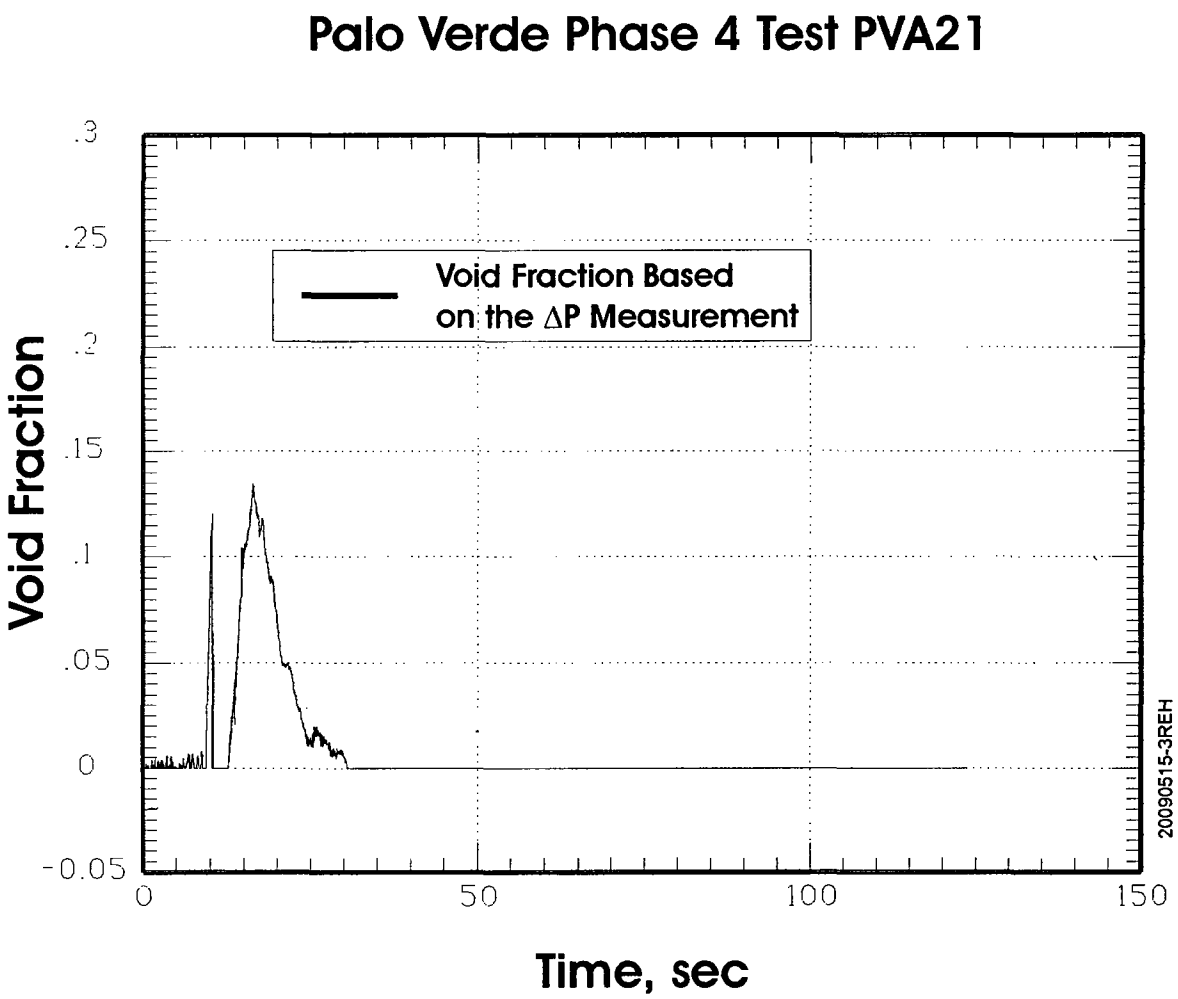

show that a separated flow pattern was never observed at the bottom of the downcomer and bubbly flow was always observed.

Given the importance of the kinematic shock, it is interesting to compare the analytical model described above to the experimental results. The test conditions of interest are an initial high point void fraction of 0.6 (after the compression to the sump pressure) in a 5 foot long, 4 inch pipe which is an initial gas volume of 0.261 ft^3. As shown in Figure 6, the downcomer was a 3 inch transparent pipe whereas the high point was a 4 inch pipe. This was done to ensure the downward water velocity exceeded the bubbly rise velocity as would be the case for the plant suction piping. Therefore, since the kinematic shock was formed in the 3 inch pipe, the Froude number in this pipe is twice that in the high point piping for the same imposed volumetric flow rate. This results in a Froude number in the kinematic shock region of 1.2. Using the approximation to the integral gives the following results for the kinematic shock behavior:

- the initial (maximum) depth of the kinematic shock is 4.8 feet,
- the maximum void fraction at the bottom of the kinematic shock equals 0.27,
- the average void fraction at the bottom of the shock region is 0.18 and
- the average gas entrainment rate is 0.037 ft^3/sec

With the calculated average gas entrainment rate, the initial gas volume would be eroded over an interval of 7.1 seconds. Comparing this with the test duration shown in Figure 9, it is observed that this calculated interval is shorter than the recorded test interval, i.e. about 15 seconds. Hence, the model developed in this report provides a conservative assessment (over statement) for the rate of gas transport to the pump. Moreover, considering the calculated maximum void fraction at the bottom of the kinematic shock region (about 0.27) and the slip ratio with a downward water velocity of approximately 3.5 ft/sec in the 3 inch diameter downcomer, combined with a bubble rise velocity of 1 ft/sec, the slip ratio is 0.71, the void fraction at the bottom of the downcomer, including the influence of buoyancy, is 0.34. Furthermore, considering the influence of the downcomer static head, which is approximately an 8 foot elevation change, to estimate the static head it is assumed that the entire vertical height has a void fraction of 0.34 and thus a mixture density of approximately 66% that of water. Therefore, the static head increases the pressure at the bottom of the downcomer to about 32.3

psia compared to the pressure of 30 psia imposed by the containment sump. This additional compression results in a final calculated void fraction of 0.32. Figure 10 shows the maximum measured void fractions at the bottom of the downcomer in the Palo Verde integrated system experiments as a function of the one-dimensional water velocity through the high point. It is observed that a value of 0.32 is consistent with the maximum peak void fractions measured in the numerous tests that were conducted. (Remember also that, at a Froude number of 0.6, some of the experiments did not result in all of the gas coming down, hence, many of the peak void fractions are less than the calculation which assumes that all of the gas is transferred to the kinematic shock.) As discussed above, the influence of the static head calculation was performed assuming that the entire vertical elevation change had a mixture density equal to 66% that of water. Because the vertically separated flow pattern at the top of the downcomer (above the kinematic shock) exhibits essentially no static head, the actual static head change is less than this value. Hence, a more realistic estimate of the average void fraction in the downcomer would be approximately 0.33.

As illustrated by the equations for the peak and average void fractions at the bottom of the kinematic shock, with the erosion of the captured gas volume at the top of the downcomer, the depth of the kinematic shock decreases with time. Consequently, the void fraction that is transmitted toward the pump from the bottom of the kinematic shock will approach zero. This is the behavior shown by the experimental void fraction measurement in Figure 9. Hence, the equations for the instantaneous erosion rate can be solved numerically to calculate the gas intrusion transient as dictated by the response of the kinematic region. However, the results for the peak and average void fractions are sufficient to characterize the global response of the two-phase system and develop a criterion for the condition(s) needed to ensure that a kinematic shock will be formed. Specifically, this criterion is sufficient to ensure that a bubbly mixture exists at the bottom, i.e. a slug bubble will not penetrate to the bottom of the downcomer.

One additional conservative aspect of the Palo Verde tests is that this configuration had a sharp elbow at the top of the downcomer. Most plant configurations use long radius elbows and these would act to maximize the volume of the stable gas bubble that could exist in the elbow. Furthermore, a long radius elbow is anticipated to also minimize the gas entrainment rate, which

Figure 10: Measured local void fractions at the bottom of the downcomer for the Palo Verde integral system scaled tests.

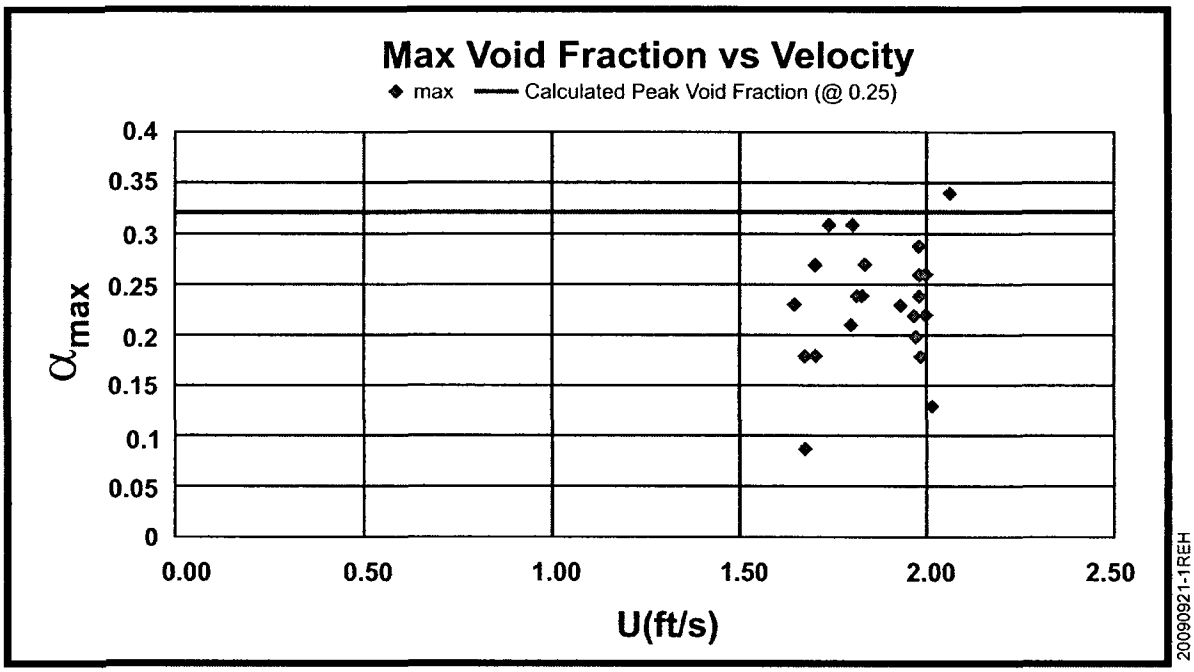

would be manifested as a lower void fraction at the bottom of the downcomer and a longer entrainment interval, i.e. a slower rate of gas intrusion to the pump suction. It is noted that the transient experimental void fraction history shown in the NEI Letter APC 09-20 (NEI, 2009) is taken from the PWROG experiments conducted at Purdue University which used long radius elbows for the various diameter test sections and lower initial void fractions in the high point piping. These values are more typical of the peak high point void fractions that would be consistent with the suction piping acceptance criteria given in Table 1. These initial conditions and configurations would generate smaller peak void fractions than those observed in the Palo Verde integrated system tests.

5.2 PWROG/Purdue Large Scale Tests

a, c

Figure 11: A schematic representation of the Purdue 12 inch diameter large scale system tests (Lin, 2009).

a, c

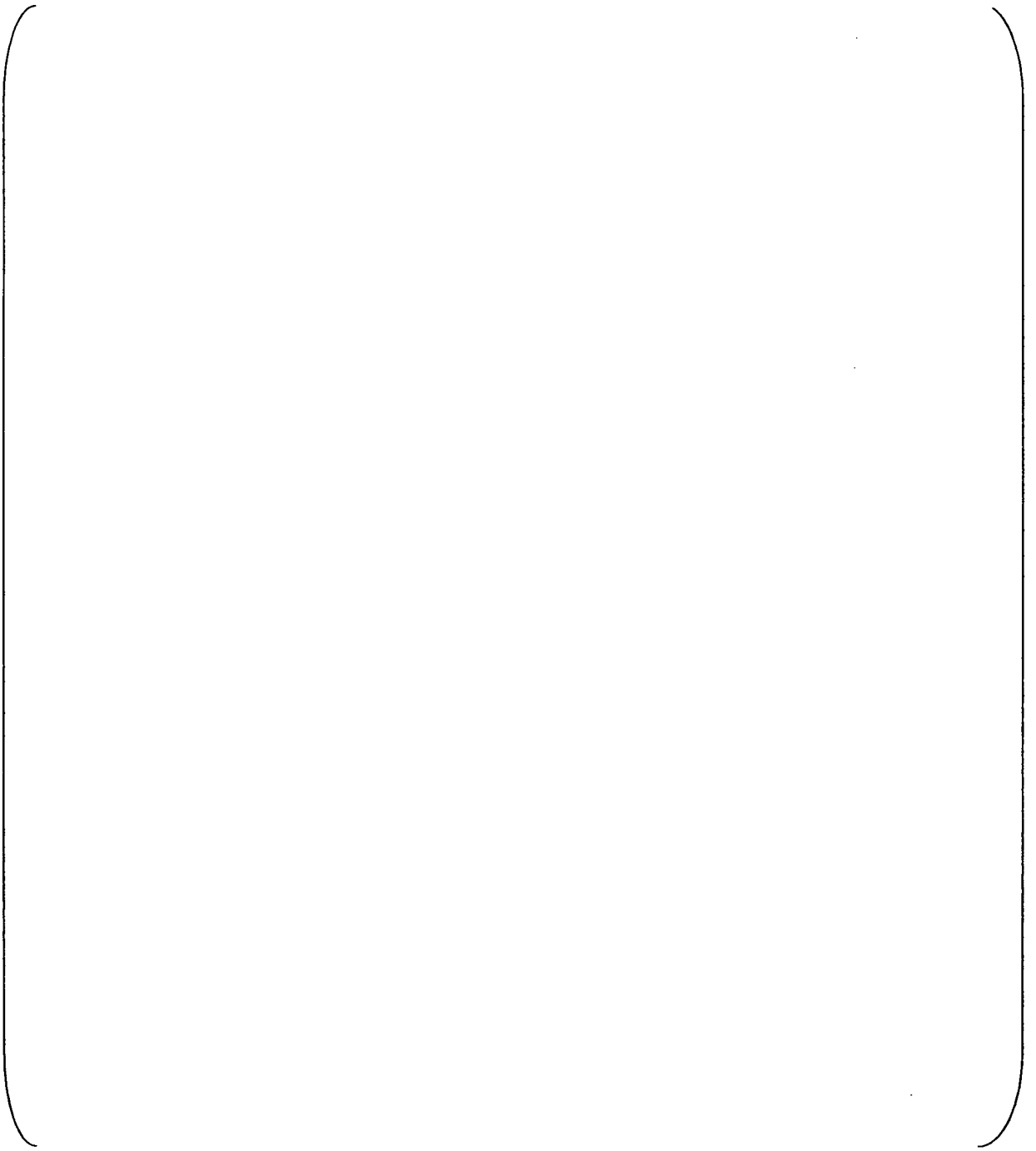

Figure 12: Calculated maximum and average downcomer void fractions at the bottom of the downcomer piping for the Purdue 12 inch large scale system tests.

a, c

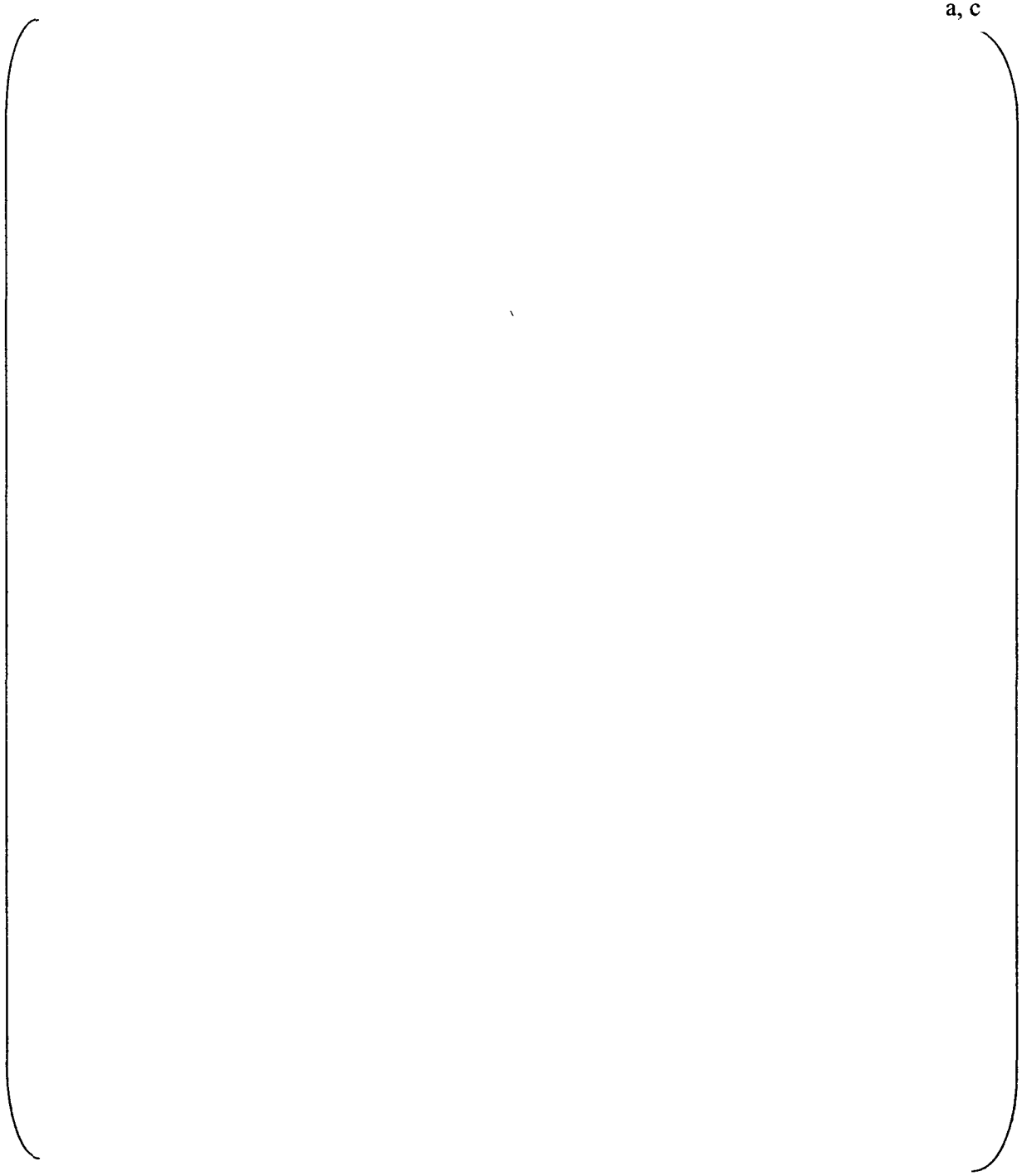

a, c

These large scale tests provide an extensive set of experimental data to further assess the details involved in the kinematic shock in the top of the downcomer, as well as other facets of the transport processes of the gas to the pump suction. This includes the behavior of the gas as it transitions from the bottom of the downcomer, through a long radius elbow, and into the horizontal piping, the influence of higher water temperatures, etc. Currently, this large scale testing program is still ongoing and thus is not addressed further in this report. However, this is an important source of information to be examined in the future to further investigate the details of the kinematic shock region and perhaps reduce some of the conservatisms in the current assessment.

Figure 13: Comparison of the integral and approximate solutions for the depth of the kinematic shock.

a, c

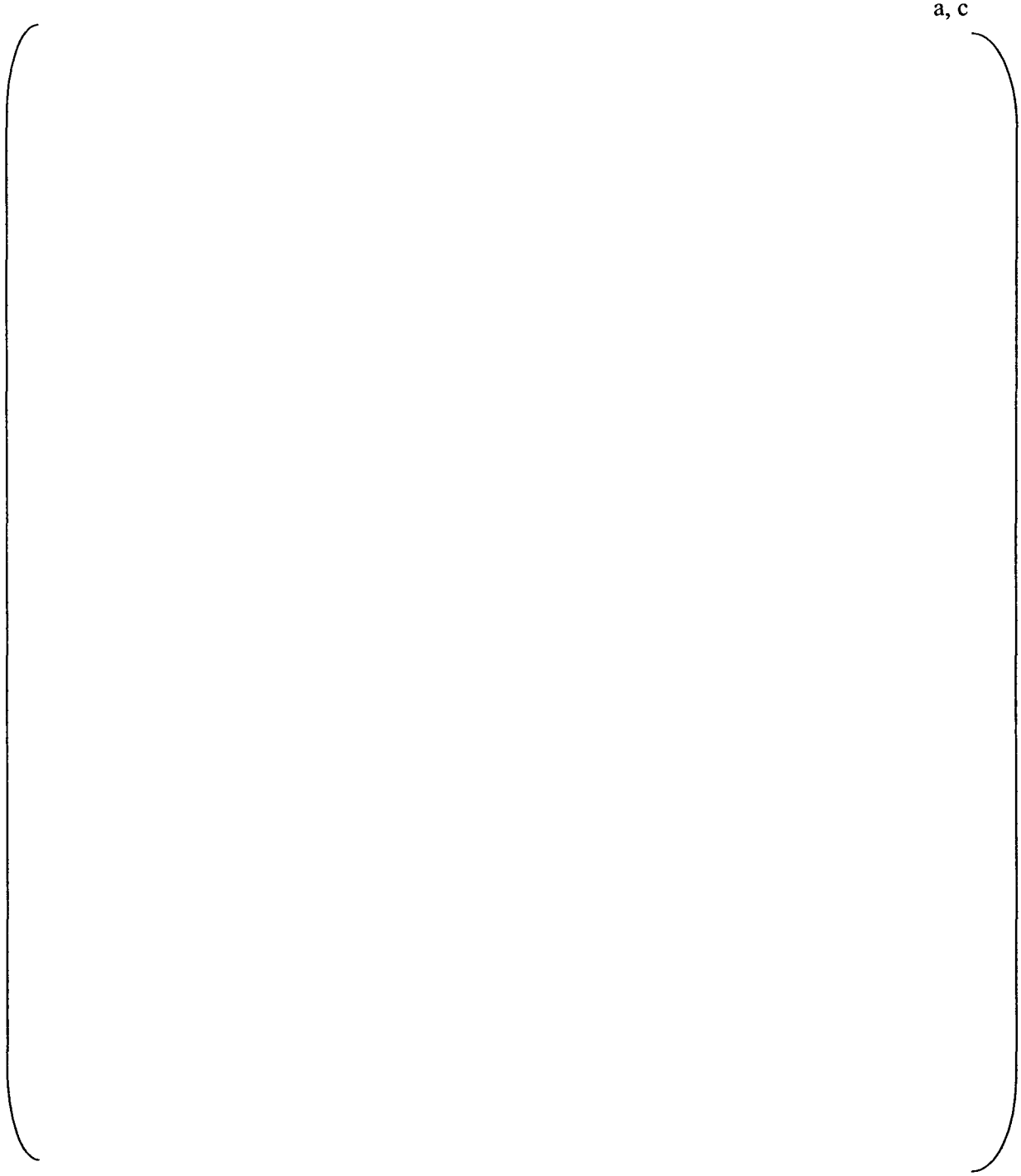

6.0 CRITERION TO ENSURE A KINEMATIC SHOCK IS FORMED

From the above comparisons with the integrated system tests, the evaluation of the depth of the kinematic shock, at its maximum value, is calculated to be approximately one-half the height of the downcomer. As discussed above, it is this height that is important in providing the transition to a water continuous, bubbly flow pattern and this is critical to the assurance of the transient pump performance, i.e. no transmittal of a slug flow configuration to the pump suction. To ensure that there is always a sufficient downcomer height to establish the necessary kinematic shock, the criterion recommended for application to plants is that the downcomer volume should be at least four times the volume of the maximum gas accumulation in the high point piping. For those piping geometries that have several steps in the vertically downward direction, the largest of these steps should have a volume that is at least four times that of the maximum accumulated gas volume. Any conditions in which the gas volume is greater than the recommended criterion should be evaluated with a detailed system specific evaluation using a transient two-phase hydrodynamic model such as GOTHIC, RELAP5, TRACE, etc.

Figures 14 and 15 illustrate generic piping configurations. Neither of the two examples shown in Figure 14 satisfy the criterion for the development of a kinematic shock, while those shown in Figure 15 do satisfy the criterion. These examples provide guidance on how to apply the criterion to plant specific configurations.

Moreover, with respect to piping configurations, it is noted that both of the experimental facilities discussed in the previous section have piping configurations that progress monotonically downward from the high point to the pump suction. This is the typical piping configuration, but some designs may have pump specific configurations where the piping elevation rises to a local high point before moving downward to the pump suction. These need to be examined with respect to potential for the gas to separate out in the local high point as it flows to the pump. The response to subsequent plant specific configurations with local high points that are water filled prior to the pump start, should consider the Froude number at the time that the gas begins to arrive at this local high point. As shown previously in this report, when the

Figure 14: Two examples of piping configurations that do not satisfy the criterion to establish a kinematic shock.

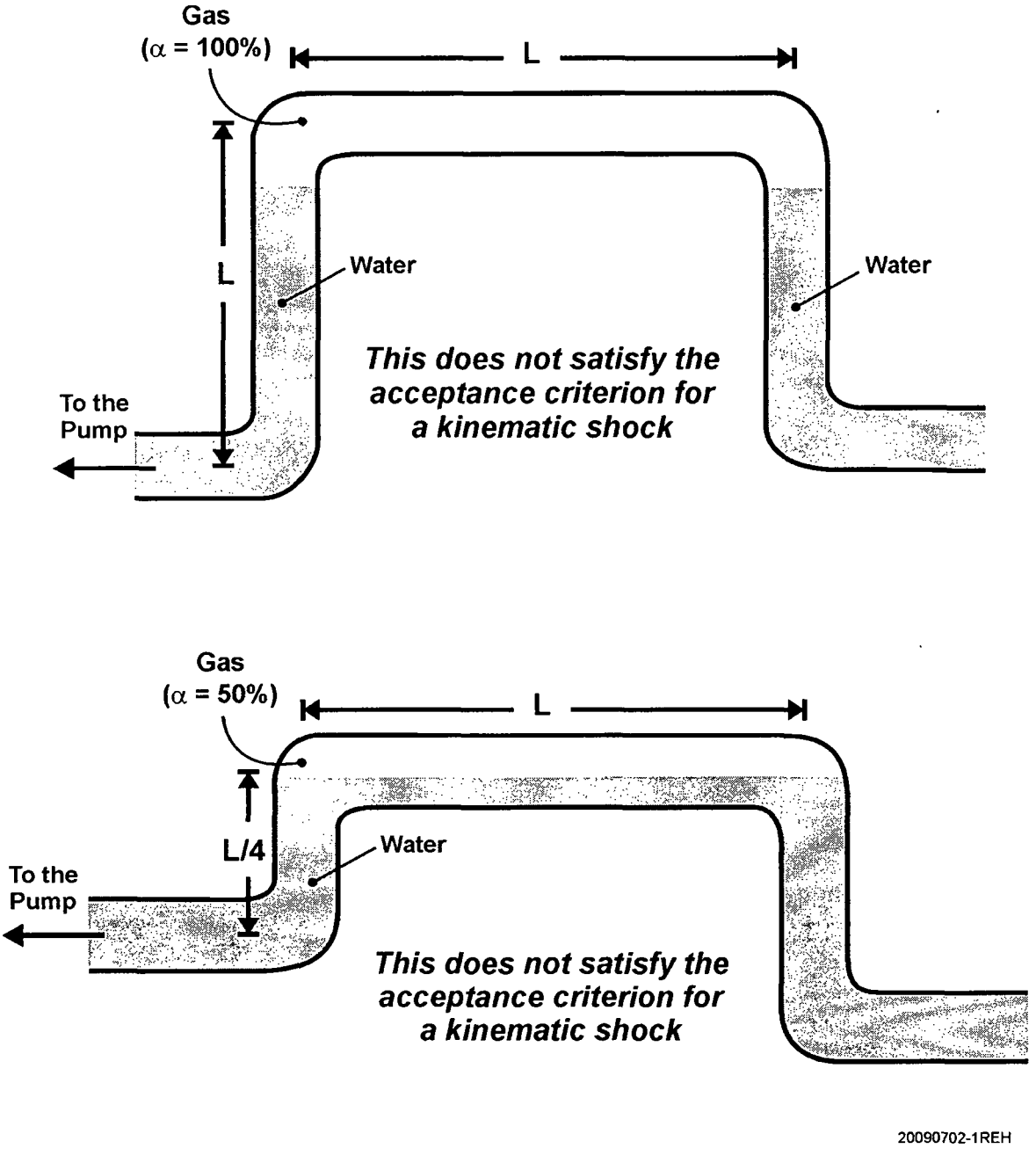

Figure 15: Two examples of piping configurations that do satisfy the simplified criterion for establishing a kinematic shock.

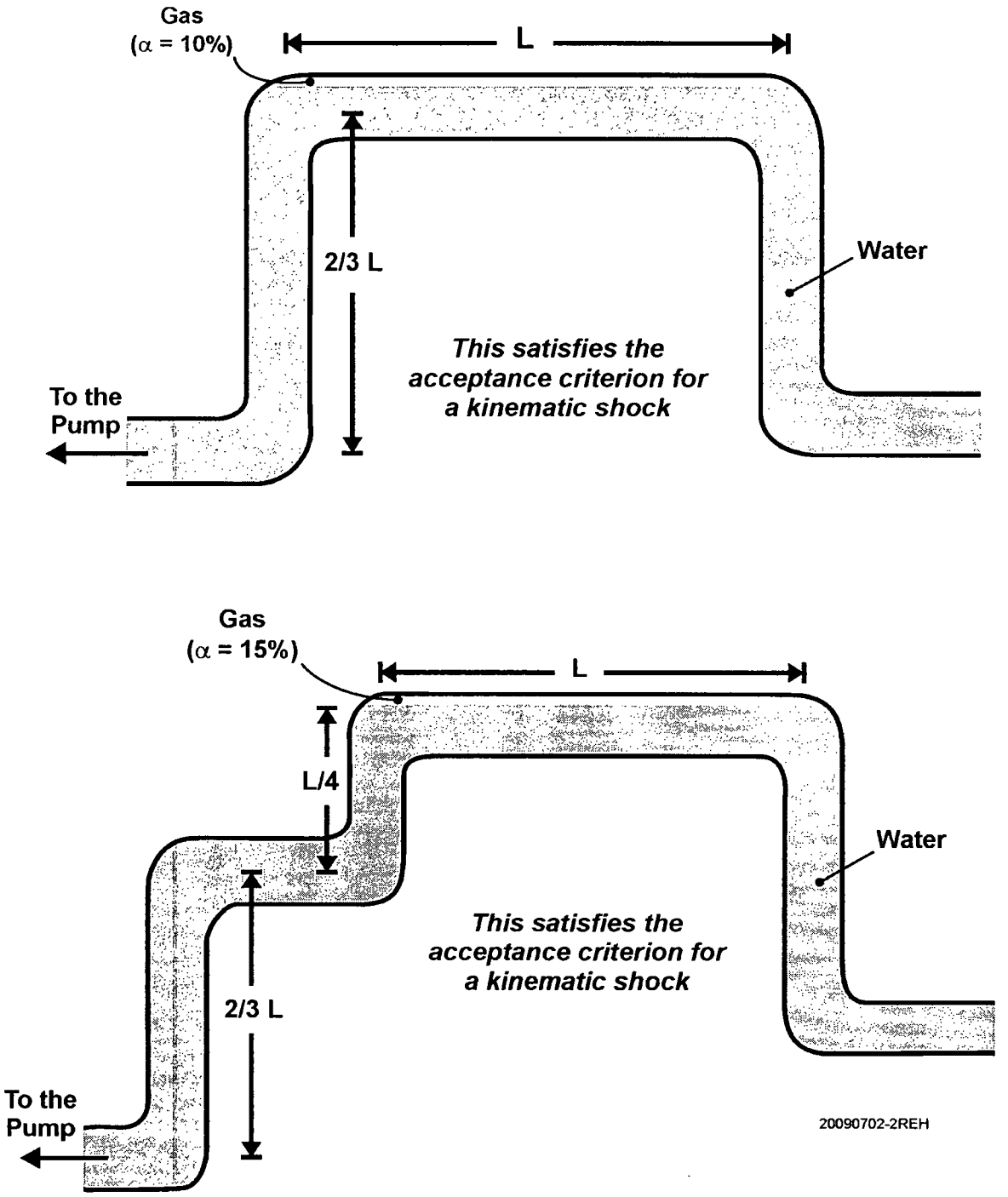

Froude number is greater than approximately 0.5, there is no significant potential for the gas to separate out, i.e. the pipe would satisfy the conditions to "run full". Hence, if the gas is transported to the high point as a bubbly mixture, it would remain as a bubbly mixture. This should be the first item considered for those designs which have such water filled, local high point configurations.

7.0 USE OF A SIMPLIFIED EQUATION

As defined in Table 1, the criteria for the allowable average gas void fractions to enter the pump suction are given in terms of a void fraction and the event duration. These criteria represent the potential challenges to the pump operation which is the volume of gas that could be accumulated in the pump, independent of the details of the void fraction being transported to the pump. Consequently, the approach focuses on the total gas volume that would not be sufficient to cause a significant decrease in the pump discharge head. However, the steady-state condition is given to represent the maximum inlet void fraction condition where the pump characteristics enable the exiting gas mass flow rate to equal the incoming rate, i.e. there is no continuing gas accumulation. This is experimentally based and comes from large scale pump tests, such as those described by Smyth et al (2006). Therefore, there is a difference in the underlying meaning of the listed values in the table.

Given the pump suction flow rate(s) (Q_s) and the existence of a bubbly flow region exiting from the bottom of a downcomer, the individual criterion can be represented as a gas volume that could enter the pump and this can be expressed as:

$$V_{gp} = Q_s \, \bar{\alpha}_p \, \Delta t \tag{30}$$

where $\bar{\alpha}_p$ (the average gas void fraction entering the pump(s)) with the duration of the event (Δt) are defined in Table 1. In essence, this is the two-phase homogeneous continuity equation where the volumetric flow rate is fixed by the nominal pump flow rate and the other parameters are given by the criteria in Table 1. For those piping configurations that have a significant elevation difference between the piping high point and the pump suction location combined with frictional and form losses that are small compared to the static head, the gas volume in the high point is given by

$$V_{ghp} = V_{gp} \left(\frac{P_p}{P_{hp}} \right) \tag{31}$$

where P_p and P_{hp} are the imposed local pressures at the pump suction and high point locations respectively. To be meaningful, this elevation difference needs to be at least 10 ft, otherwise the difference in the static head is not significant. Also, the higher the pressure P_p the less sensitivity there is to the static head. Most importantly, the downcomer needs to have a sufficient volume to capture the gas volume in the top of the downcomer to ensure the formation of a kinematic shock. As discussed previously, this kinematic shock process controls the erosion rate of the gas volume, and hence, the rate at which the gas volume is transported to the pump(s) suction(s). In essence, the assurance that no gas slug can be transmitted to the pump suction rests solely on having a piping configuration with the necessary properties to establish a kinematic shock in the downcomer piping.

As discussed in Sections 1 through 5 the homogeneous structure of the equation and the assumptions in this simplified equation are consistent with the available technical basis. Specifically, this includes:

- the two-phase flow pattern is one of bubbly flow, not slug flow and
- the gas transport is a short duration event for the pump in question.

8.0 IMPLEMENTATION OF THE CRITERIA

8.1 Implementation of the Simplified Equation

The first step in implementing the simplified evaluation criteria is to ensure that the accumulated gas volume is within the constraints to form a kinematic shock to prevent gas slugs from being transmitted to the pump suction. Therefore, ensure that the high point gas volume is limited to a maximum value of one-fourth of the downcomer piping volume.

Next the transient criteria in Table 1 need to be applied to ensure that these are not exceeded. For example, consider the scaled experiments reported by Hammersley et al. and the criteria in Table 1 for an operating point that is close to the Best Efficiency Point (BEP), i.e. between 70% and 120% of BEP. The total suction flow rate for a Froude number of 0.6 is 78 gpm (0.174 ft^3/s), hence the gas volume entering the pump suction for a single stage pump with a void fraction of 0.05 for a duration of 20 seconds would be limited to:

$$V_{gp} = (0.174)(0.1)\,5\,\text{secs} = 0.087\ ft^3 \qquad (32)$$

This corresponds to 40% of the high point volume between the butterfly valves. However, as discussed by Hammersley et al, one of the important observations in the $1/6^{th}$ and $1/3^{rd}$ scaled tests was that the suction header pipe configuration resulted in a vortex being generated at the High Pressure Safety Injection (HPSI) pump suction take-off from the suction header. This resulted in virtually all of the gas being transported to this multi-stage pump. Using this observation to apply the results to the reactor system, the information in Table 1 for the multi-stage, stiff shaft (CA) pump is applicable and corresponds to a gas void fraction of 0.20 for 20 seconds. (To make the following point, it is not necessary to complicate the evaluation by considering how the variable time scales in the experiment.) More importantly, the scaled HPSI flow rate is 12.8 gpm (0.0285 ft^3/sec) and evaluating the size of the gas volume using the pump specific parameters in the criterion a volume of 0.114 ft^3 is calculated. This concludes that a considerably larger volume can be tolerated if the gas is essentially all transported to the HPSI pump. This observation makes the important point that with a header configuration, the multiple

pump suction locations could experience a non-uniform distribution of the gas transport to the different pumps. If there are scaled experiments or detailed analyses that demonstrate this distribution, the acceptance criteria could be implemented on a pump specific basis with this distribution/partitioning of the gas transport included. Conversely, in the absence of scaled experiments, or detailed analyses, the analyses should be performed assuming the entire high point gas volume is transported to each of the pump suction locations with credit being taken for the increase in the static head. The limiting case for the acceptance is the pump with the smallest tolerable gas volume.

If there is no header configuration for the system being evaluated, the calculation is straightforward in terms of the manner of implementation. Specifically, the pump suction volumetric flow rate is used along with the pump specific acceptance criteria from Table 1 to determine the tolerable accumulated gas volume with the static head increase again being credited.

8.2 PWR Configurations

As noted above, the first plant specific feature to be addressed in the application of the simplified criteria is to ensure that the accumulated gas volume is not sufficient to overwhelm the downcomer. Figure 13 provides two examples of piping configurations that do not satisfy the criterion and Figure 14 shows two examples of piping geometries that do satisfy the criterion.

Figure 1 illustrates a header like configuration that is used in most PWR suction piping configurations to transport the borated water from the storage tank, or the containment sump, to the pump suction location. With the header configuration, the pump flow condition for a specific type of accident condition, i.e. small break, medium break or large break LOCA, needs to be addressed in terms of the total flow rate through the suction piping. Hence, the gas ingested by all of the pumps needs to be determined before assessing the gas transport. Specifically, if a small LOCA is being considered, the elevated RCS pressure could be sufficient to prevent the low pressure systems from injecting, and therefore, the suction flow rates for these pumps would only be the mini-flow rates. Furthermore, depending on the containment design and the specific

accident conditions, the containment pressure may, or may not, be sufficiently high to initiate the containment sprays. Hence, the total volumetric flow rate for the suction piping would be the injection flow from the high head systems, the mini-flow for the low head systems and most likely the containment spray flow. This would be the total demand flow through the suction header configuration. If this flow rate results in a Froude number in the piping high point that is less than 0.3, there would be no significant gas transport to the pump suction location and the analysis does not need to address this set of conditions any further.

Should the specific accident conditions result in a depressurized RCS, the flow rate through the header would be considerably increased since the low head systems would be injecting. Furthermore, the containment spray systems would likely be activated (this is system specific) and this suction flow would be added to the flow through the header piping. Under these conditions, the suction flow rate demanded by each pump/system needs to be calculated for the most limiting accident conditions to determine the conditions that limit the gas accumulation. As noted above, this can vary with the header configuration and also with the pump operating point in relationship to the BEP. Considering first the header configuration, the gas volume for each pump should be calculated and, unless there are specific experiments or analyses that specify the distribution/partitioning of gas to the individual systems/pumps, the analysis should assume that all of the gas could flow to a single pump. The system/pumps with the minimum calculated tolerable gas volume determine the maximum acceptable gas volume for the suction piping. This volume can then be corrected for the static head to assess the volume(s) in the piping high point(s). A further increase could be calculated to include the volume of the stable gas bubble that could reside in the downstream piping elbow. As explained above, this is generally a small volume compared to that which is transported to the pumps and may be neglected as a small conservatism in the application of the acceptance criteria. This total volume then represents the extent of gas that could be accumulated in the piping high point without challenging the acceptance criteria presented in Table 1.

9.0 OPERATING CONDITIONS

As noted at the beginning of this report, the objective of these evaluations is to determine those conditions that are required to ensure that gas slugs are not transmitted to the pump suction. The occurrence of a kinematic shock in the downcomer piping is the mechanism that causes the transition from a vertically separated flow to a bubbly flow pattern, and as such prevents the transmission of gas slugs. A criterion has been developed (the downcomer volume is at least 4 times the volume of the accumulated gas volume) to characterize the requirements for the kinematic shock to form. Given this criterion, there are a few conditions that should be discussed with respect to the pump conditions that are removed from the BEP operating point.

9.1 Conditions Near the BEP Conditions

Table 1 is a conservative representation of this complex set of physical processes, i.e. the criteria in Table 1 characterize the entrainment of the gas volume as a process that occurs within an interval that is shorter than 10 seconds when the pump is operating between 70% and 120% of the best efficiency point. For example, from the experimental measurements discussed in the previous sections, as well as that represented in NEI Letter APC 09-20, it is observed that the duration of the gas transport to the pump suction location is longer than the intervals listed in Table 1. From this alone, the technical basis shows that the evaluation criteria are a conservative representation of the mechanistic transport processes.

9.2 Conditions Outside of the BEP Conditions

For those conditions that are removed from the region defined as 70% to 120% of the BEP operating point, the two separate considerations to be addressed depend on whether the operating point is below and above the BEP operating range. For those operating conditions that are less than 70% of the BEP, the pump demand flow rates are substantially less than the nominal values typical of the BEP conditions. In general, these are flow rates considered for smaller break LOCA events where the RCS would, or could, remain at an elevated pressure. The gas transport criteria provides for considerably lower flow rates in that the evaluation first needs to determine

if the Froude number for this suction demand is greater than 0.3. If not, there is no potential to pull the gas downward through the vertical downcomer piping, i.e. no gas would be transported to the pumps. (No gas transport at low Froude numbers was observed in the experiments reported by Hammersley et al.) If the Froude number is greater than 0.3 but less than 0.5, the criterion developed above in terms of a stable bubble flow should be evaluated to assess the extent of gas that would remain stable in the piping high point and downturned elbow like that shown in Figure 16. Any gas volume in excess of this value should then be assessed as being entrained and transported to the pump. However, since the velocity is reduced considerably for these conditions, this entrainment interval should be considered at 10 seconds instead of the 5 seconds considered for the operating near the BEP. If the Froude number is greater than 0.5, the gas transport should be evaluated in the same manner as those operating conditions that are close to the BEP point.

For those conditions in which the operating point is greater than 120% of the BEP, the flow rates are approaching the run-out conditions and are not challenged by pumping against an elevated RCS pressure. Under these conditions, the downcomer volume criterion for the establishing a sufficient kinematic shock in the downcomer is also applicable. Furthermore, the evaluation of the various pumps can rely on the large scale pump tests performed by Arizona Public Service (APS) for the multi-stage and single-stage pumps used in the Palo Verde design. (Smyth et al., 2005). Those full scale experiments with a multi-stage High Pressure Safety Injection pump demonstrated that the multi-stage pump operated over many tens of seconds with a steady-state imposed suction flow rate having a mixture void fraction in excess of 20% entering the pump. Furthermore, the single-stage pump demonstrated that it could operate over many tens of seconds with the imposed suction flow having a steady-state void fraction of 5% entering the pumps. Consequently, these experiments provide an important full scale demonstration of the behavior that is expected at these higher operating flow rates. While these tests did not cover the entire range of possible operating conditions for ECCS pumps, they are an essential part of the technical basis to be used for:

Figure 16: Possible configuration for low Froude number flows.

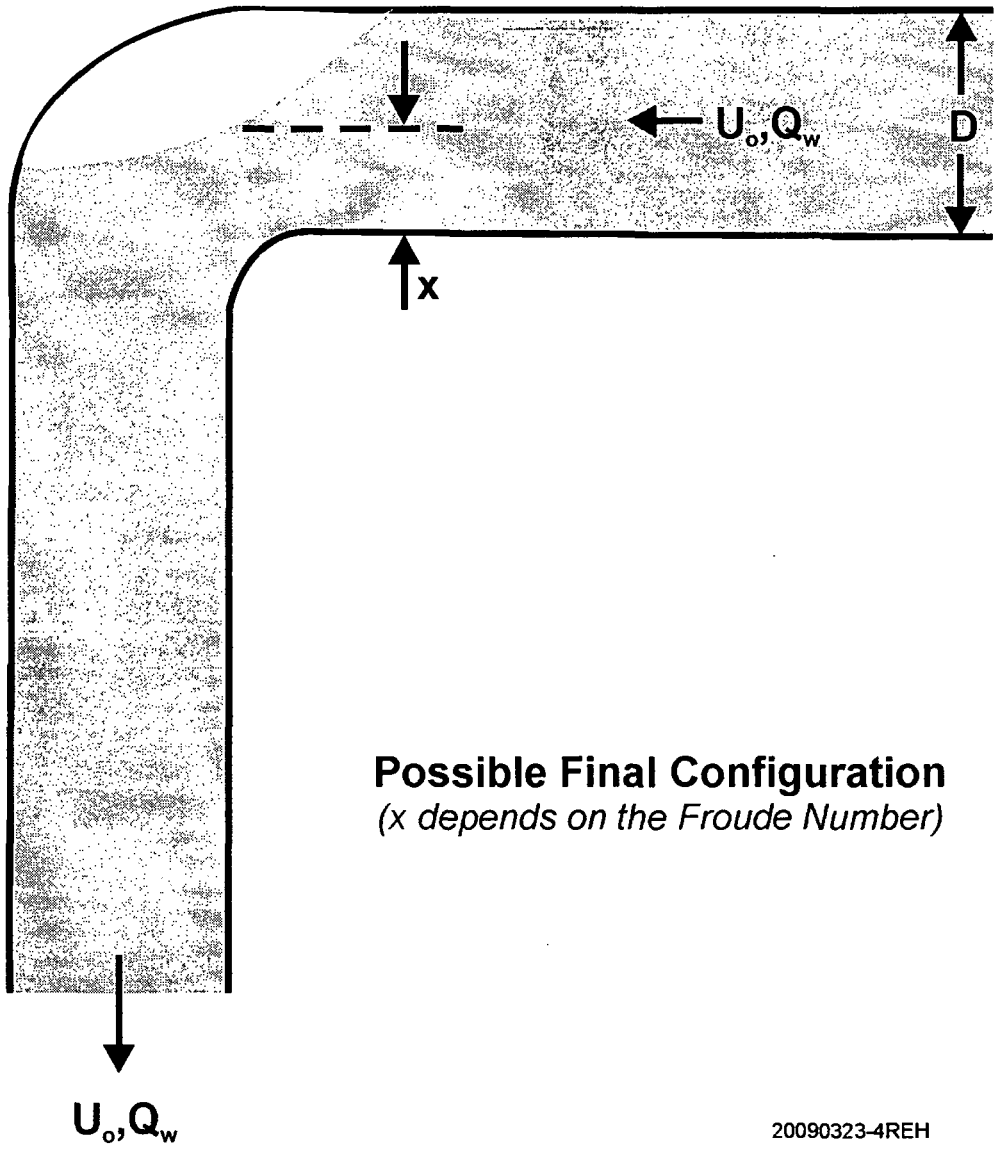

- the pumps that experience the operating conditions tested and
- a basis for extrapolating to other pump operating conditions that are at higher flow rates than 120% of the BEP point.

With all of the accident and operating conditions that are considered, that which has the most limiting gas volume will determine the maximum acceptable gas volume in the high point of the piping. This includes the considerations that, depending on the piping design, all of the gas volume could potentially be transported to a single pump, or set of pumps.

10.0 SUMMARY AND CONCLUSIONS

10.1 Summary

Through these evaluations, those characteristics associated with the possible challenges to the pump suction demands demonstrate that the principle process relating the potential challenge to the volume of gas accumulated in the high point is the action of pulling the existing gas volume toward, and into, the downcomer piping. At this location, the two-phase mixture must develop a configuration that enables water to be supplied from the upstream water source at a volumetric flow rate equal to the pump suction demand. As this develops, the formation of a kinematic shock in the downcomer is necessary to ensure that a bubbly two-phase mixture is formed. This will prevent the transmittal of a continuous gas slug toward the pumps. A criterion has been constructed to ensure that the downcomer is sufficient to form such a kinematic shock, i.e. the downcomer volume must be at least 4 times the volume of the gas accumulated in the piping high point.

The extent that the gas volume is pulled into the top of the vertical downcomer pipe at this condition determines the extent of the gas volume and void fraction that would eventually be entrained into the flow stream to the pumps. For the evaluation criteria, the extent of this entrainment interval is taken as a conservative representation of the time over which entrainment was experienced in the integral scaled tests performed for the Palo Verde ECCS suction piping.

For those conditions operating away from the BEP operating range, the conditions for the lower flow system can utilize the combination of the gas that can remain in the suction header under this reduced flow state along with a longer entrainment interval since the velocity would be correspondingly reduced. For those operating conditions with a higher flow rate than the BEP operating range, the technical basis is derived from the full scale Palo Verde experiments for single-stage and multi-stage pumps.

In summary, each of the components of the evaluation criteria for determining the extent of void fraction entering the pump suction has a substantial technical basis in large scale and full

scale experimentation as well as the basic understanding of two-phase flow for these transient behaviors. The important features that comprise the suction flow criteria are summarized in Table 3 along with the corresponding technical basis for each feature.

Table 3

Technical Basis for the Controlling Physical Processes

Important Features Comprising the Criteria	Technical Basis
1. The gas volume is pulled toward the downstream elbow.	Palo Verde integral system scaled tests.
2. A two-phase flow pattern is established with water flowing under some of the gas at the top of the elbow and the remainder of the gas is pulled into, and collected in, the top of the downcomer.	Palo Verde integral system scaled tests and analytical calculations.
3. A kinematic shock is formed at the top of the downcomer that transforms the vertically separated flow patterns into a bubbly flow pattern.	The Palo Verde integral scale tests and the preliminary results from the PWROG Purdue tests.
4. At the BEP point all gas that is entrained is removed in 5 secs.	A conservative representation of the Palo Verde integral system scaled tests.
5. In the range of 70% to 120% BEP, the pumps can operate well for an average void fraction of 5% for 20 secs, 20% for 20 secs.	 APS single-stage pumps. APS multi-stage pumps.

10.2 Conclusions

1. The suction flow developed by the pumps causes the gas volume to be pulled toward, and perhaps into, the downcomer piping.

2. The depressurization of the gas volume due to the pump start is only that needed to cause the upstream volumetric supply flow to equal the suction demand flow. For typical piping this is a very small pressure decrease, i.e. approximately 1 psi.

3. For internal flow Froude numbers less than 0.3, the water will flow under the gas volume and there will be no significant gas volume transported toward the pump(s). As the Froude

number increases toward a value of approximately 0.6, the extent of gas that can remain above the water is small with the rest of the gas being pulled, or pushed, downstream into the top of the downcomer pipe.

4. As long as the downcomer volume is more than four times larger than the accumulated gas volume, a kinematic shock will develop in the top of the downcomer. This dynamic flow process prevents the formation of slug bubbles and results in the formation of a bubbly flow condition at the bottom of the downcomer. It is this water continuous mixture that would be pulled downward toward the pumps. As demonstrated by the Palo Verde integral system tests, at the bottom of the downcomer, this bubbly flow has a maximum void fraction of approximately 0.25 for a large initial gas volume in the piping high point. This maximum void fraction is reduced for smaller initial gas volumes.

5. The representation of the effective gas transport to the pumps in terms of average void fraction and duration of the gas transport as given in NEI (2009) are conservative representations of the transport process. When calculated using the product of these two variables, the resultant gas volume is a conservative (smaller) estimate of the gas volume that could be tolerated by the pump(s).

6. Depending on the suction piping configuration, there can be a significant elevation difference between the system high point(s) and the pump suction locations. For most systems the static head is large compared to the frictional and form losses associated with the flow. The static head associated with this elevation difference (typically tens of feet) would cause a reduction in the gas void fraction as it is transported to the pump(s).

7. With the bubbly flow configuration at the bottom of the downcomer, the combination of the integral scaled experiments along with the full scale pump tests for single stage and multi-stage pumps, the acceptance criteria for individual pumps can be assessed using the simplified equation and the influence of the static head increase discussed in this report.

11.0 REFERENCES

Bin, A. K., 1993, "Gas Entrainment by Plunging Liquid Jets," Review Article No. 43, Chemical Engineering Science, 48, pp. 3585-3630.

Biri, A. K., 1988, "Gas Entrainment by Plunging Liquid Jets", VDI-Forschungsh, 648 88, 1-36.

Brennen, C. E., 2005, Fundamentals of Multiphase Flow, Cambridge Press, p. 308.

Epstein, M. and Fauske, H. K., 1989, "The Three Mile Island Unit 2 Core Relocation - Heat Transfer and Mechanism," Nuclear Technology, 87, pp. 1021-1035.

Hammersley, R. J. et al., 2006, "Scale Model Testing of Air Transport Through Pump Suction Piping," 9th NRC/ASME Symposium on Valve, Pump and Inservice Testing, Washington, D.C., July 2006.

Lin, A., 2009, Presentation at the PWR Owners Group Fourth International Technical Workshop, Brussels, Belgium, September 2-3.

Nuclear Energy Institute (NEI), 2009, NEI Letter APC 09-20.

Smyth, G., 2006, "Emergency Core Cooling Pump Performance with Partially Voided Suction Conditions," 9th NRC/ASME Symposium on Valve, Pump and Inservice Testing, Washington, D.C.

Van de Donk, J. A.C., 1981, "Water Aeration with Plunging Jets", PhD, thesis, Technische Hogeschool Delft.

Wallis, G. B., 1969, One-Dimensional Two-Phase Flow, McGraw-Hill Book Company, New York.

Wallis, G. B., et al., 1977, "Conditions for a Pipe to Run Full When Discharging Liquid into a Space Filled With Gas," Transactions of the ASME, Journal of Fluids Engineering, June, pp. 405-413.

Westinghouse, 2006, "Testing and Evaluation of Gas Transport to the Suction of ECCS Pumps," WCAP-26631-NP, Rev. 0, Westinghouse Electric Company Report to the PWR Owners Group.

APPENDIX A

Bubble Volume and Height Calculation

The analysis in this appendix relates the bubble volume (and void fraction) to either a known water level or a known chord length of the pipe diameter. (The chord length is the bottom of the gas volume (void) as illustrated in Figure A-1.) Note the bubble height in the result section is given by the pipe radius minus the water level. First, the bubble cross-sectional area is computed using Eq. A-1. Note that to solve for h in Eq. A-1, an iterative method needs to be used, since h cannot be solved for explicitly. The results are shown in Figure A-2 in terms of a plot of A_b/A_o vs. h/D which can be used as a lookup figure. (Note also that between void fractions of 0.15 to 0.85 the curve is almost linear.)

$$A_b = r^2\left(\beta - \frac{\sin 2\beta}{2}\right) = r^2\left(\cos^{-1}\left(\frac{h-r}{r}\right) - \frac{\sin\left(2\cdot\cos^{-1}\left(\frac{h-r}{r}\right)\right)}{2}\right) \qquad \text{(A-1)}$$

where, r = inside radius of the pipe,

β = angle as presented in Figure A-1,

h = water level height,

$\cos\alpha = \left(\frac{h-r}{r}\right)$, and

A_b = cross-sectional area of the bubble.

Once A_b is known, the bubble volume and void fraction at the high point are calculated using Eqs. A-2 and A-3.

$$V_b = A_b \cdot L_{HP} \qquad \text{(A-2)}$$

where, V_b = bubble volume, and

L_{HP} = length of high point

Figure A-1: Cross-sectional view of a collected gas volume (void) in a horizontal pipe section.

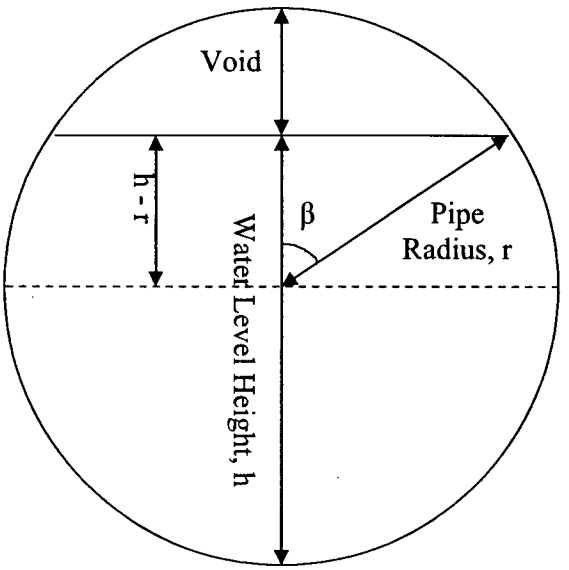

Figure A-2: Void fraction vs. the ratio of water level height to the pipe internal diameter.

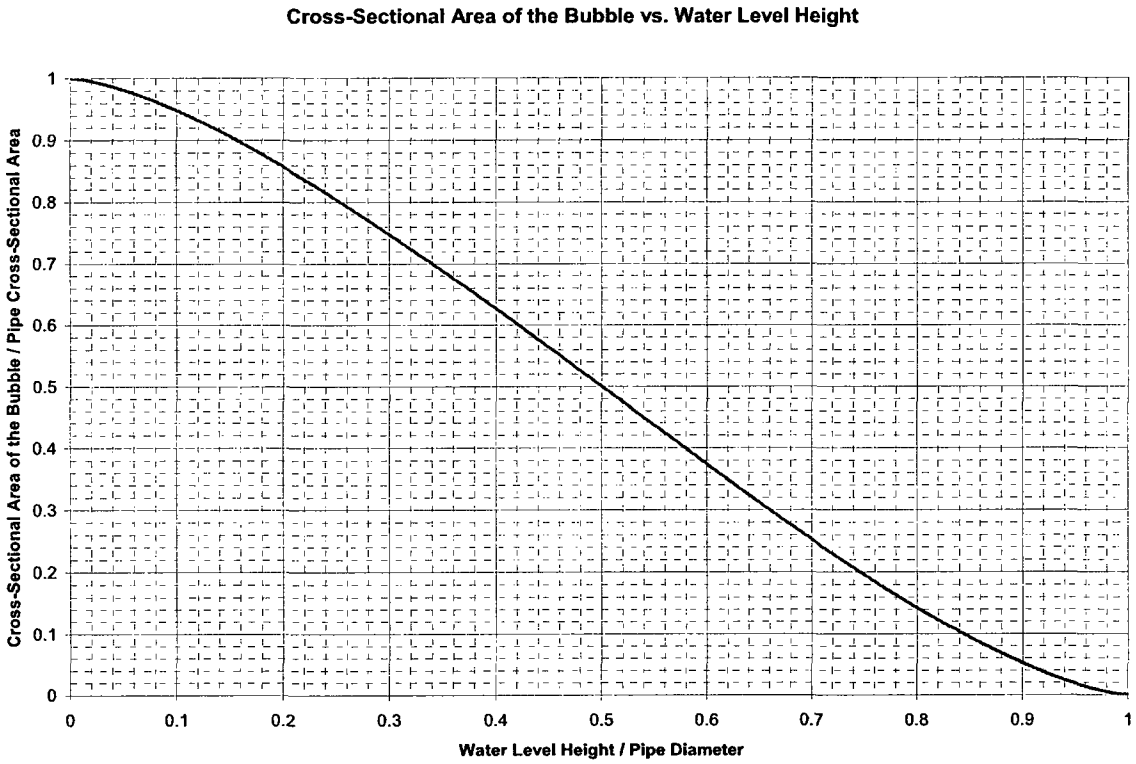

$$\alpha_{VF} = \frac{V_b}{A \cdot L_{HP}} \tag{A-3}$$

where, α_{VF} = void fraction at the high point, and

A = cross-sectional area of the pipe.

For those conditions where the width (chord) of the gas-water interface is know, the chord has a length of

$$\text{chord} = 2r \sin\beta = 2r \sin\left[\cos^{-1}\left(\frac{h-r}{r}\right)\right] \tag{A-4}$$

or

$$\beta = \sin^{-1}\left[\frac{\text{chord}}{2r}\right]$$

Once β is calculated, the gas volume is determined from Eq. A-1. Figure A-3 shows the void fraction as a function of the ratio of the chord length to the pipe internal diameter.

Figure A-3: Void fraction vs. the ratio of the chord length to the pipe internal diameter.

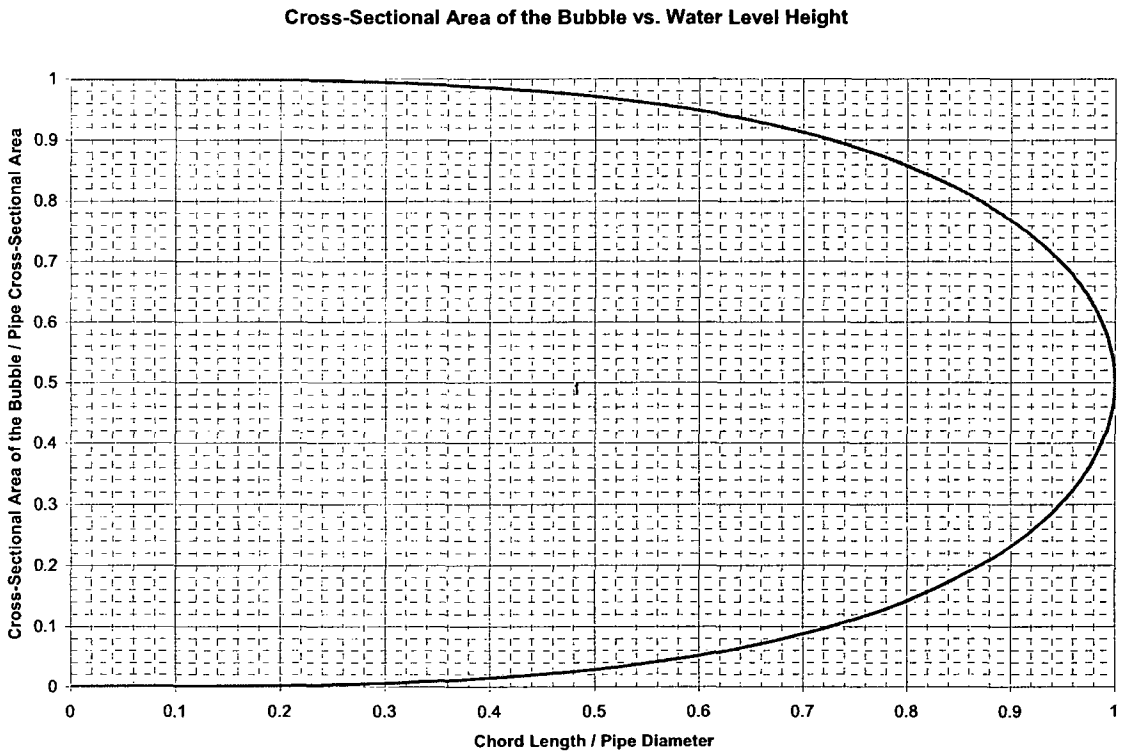

APPENDIX B

Integral Gas Transport Experiments

The experiments reported by Hammersley et al. (2006) described the gas transport behavior for the gas volume in a completely voided piping segment being transported downward through a vertical pipe (downcomer) and into a horizontal suction header for the ECCS pumps. While the length of the downcomer pipe was determined from (a) the design of the Palo Verde sump suction piping and (b) the scale of the experimental facility, the test results demonstrate that this downcomer is of sufficient volume to enable the development of a kinematic shock to transition the separated flow configuration in the piping high point into a bubbly flow pattern in the bottom of the downcomer.

Figure B-1 illustrates the general concept of the experiments and Figure B-2 is a schematic description of the complete experimental configuration including the instrumentation. In these experiments, the initially voided 5′ long 4″ ID pipe was isolated from the upstream higher pressure water source and the downstream downcomer piping by butterfly valves. To initiate the gas transport transient, these two isolation valves were opened simultaneously with opening times that ranged from 10 to 20 seconds depending upon the test. Given the characteristics of the butterfly valves, these were sufficiently opened within 3 seconds to pressurize the gas volume to essentially the pressure of the upstream water source and to begin the transport of gas into the downcomer pipe which created the kinematic shock behavior discussed in the body of the report. Since most of the piping was transparent, the gas transport behavior was recorded on digital video cameras and the gas void fraction near the bottom of the downcomer was monitored by recording the differential pressure at the bottom of the column. This pressure differential compares the static head in the bottom of the downcomer to that for an all water column of the same height. Consequently, for the small frictional pressure losses that are typical of the test conditions' the magnitude of the pressure differential is equal to the density differences over this height as described by:

$$\Delta P = \Delta\rho gh = \left(\rho_w - \left((1-\alpha)\rho_w + \alpha\rho_g\right)\right) gh$$

Figure B-1: Schematic of the test facility reported by Hammersley, et al. (2006).

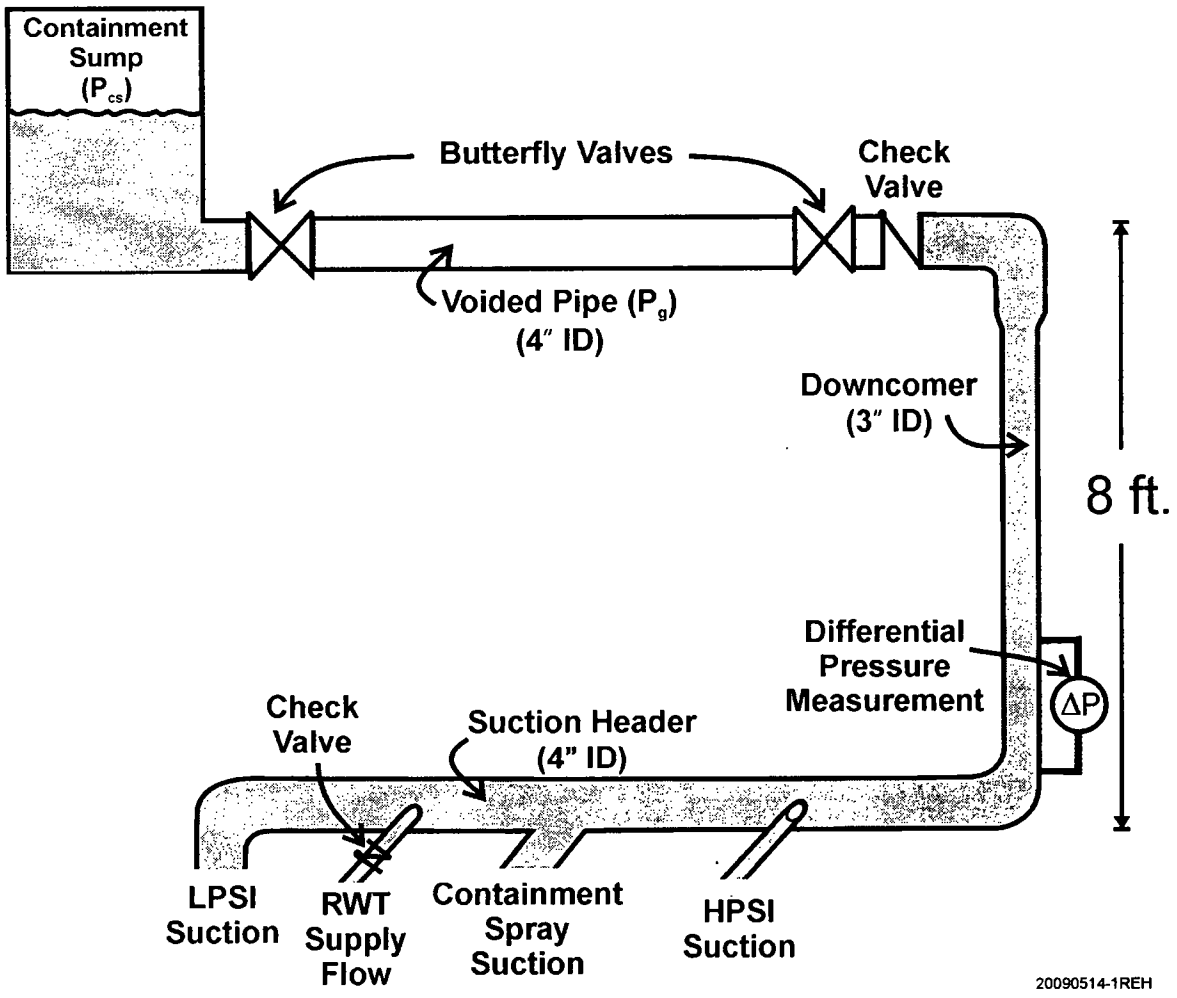

Figure B-2: Phase 2 test configuration 2C for post-RAS air intrusion (taken from Hammersley et al., 2006).

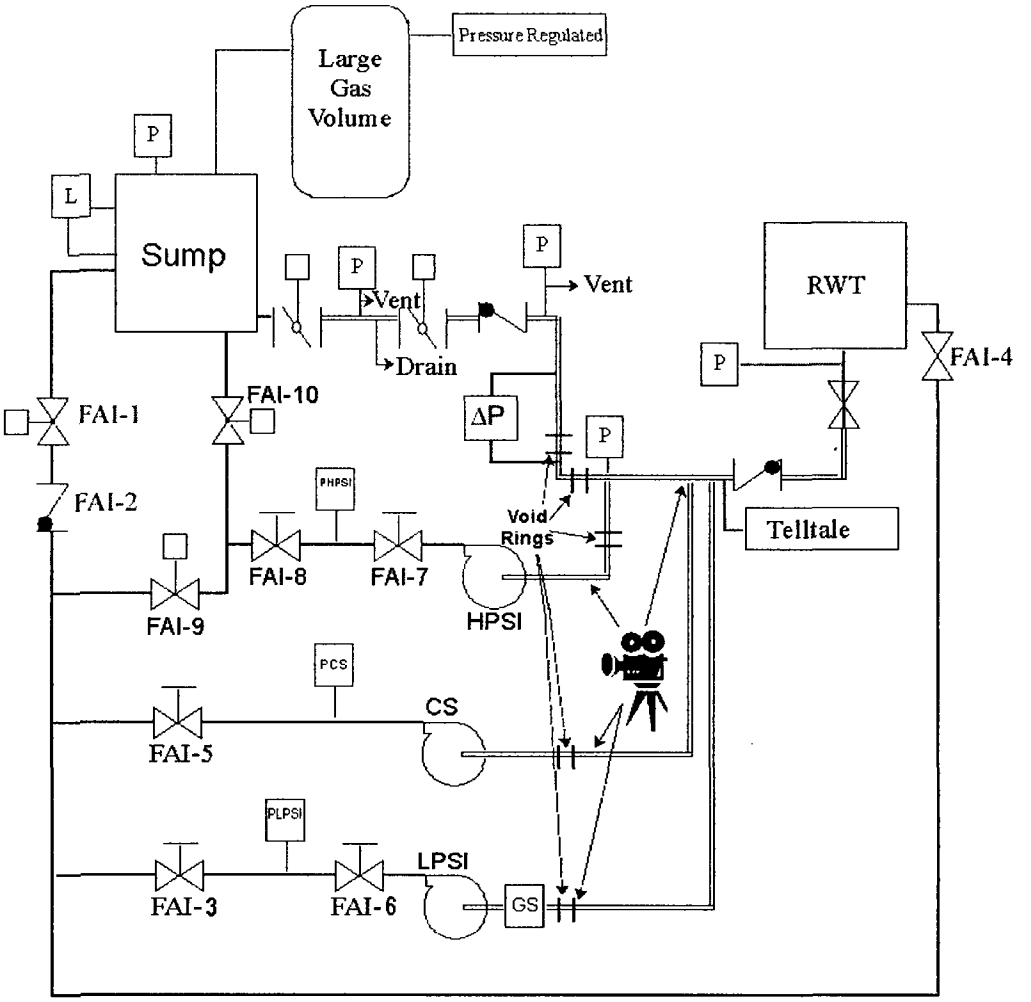

PCS / PLPSI / PHPSI	=	Turbine Flow Meter
P	=	Pressure Measurement
ΔP	=	Differential Pressure Measurement
GS	=	Gas Separator
L	=	Water Level

Notes

- Double line pipe to be transparent.
- Digital movie cameras to record flow patterns at key locations, i.e., vertical downcomer, horizontal header for the three pumps, and branch lines.
- Telltale to confirm check valve position.

In this expression, the variables are described as follows:

- g is the acceleration of gravity,
- h is the height differential over which the pressure difference is recorded,
- α is the average void fraction of the two-phase mixture,
- ρ_g is the density of the gas, and
- ρ_w is the water density.

Since the water density is two orders of magnitude greater than that of the gas for the conditions in the experiment, this expression reduces to

$$\alpha = \frac{\Delta P}{\rho_w g h}$$

Table B-1 lists the observed peak void fractions in the test runs as a function of the Froude number in the experiment. This shows that a value for the maximum void fraction of approximately 0.23 at the bottom of the downcomer is a reasonable representation of the peak values when the Froude numbers are approximately 0.6. It is noted that some of the peak void fractions tend to become larger as the Froude number is decreased. In particular, this is noted for runs PV222 and PV229, which have values of 0.48 and 0.46 respectively. As the Froude number becomes less, the downward velocity at the bottom of the downcomer can approach the bubble rise velocity. In this condition, the void fraction interpretation needs to be cognizant of the influence of buoyancy.

As part of the evaluation of these experiments, the measured void transients at the bottom of the downcomer were evaluated in terms of the calculated gas transported to the pump suction header piping compared to the initial gas inventory that was resident between the two butterfly valves. Figure B-3 illustrates one of the measured void fraction transients for test PVA22 and shows that this reaches a maximum value of 0.21 with a total transient lasting approximately 20 seconds. With the measured void fraction, the gas mass flow rate (W_g) can be calculated for each measurement point and integrated over the entire transient. The gas mass flow rate is given by:

Table B-1

Phase 2 Configuration 2A Test Results and Observations

Test Name	Test Matrix No.	$Q_1 + Q_2 = Q_{TOT}$	Froude Number	Maximum Void Fraction Downcomer	Comments
PVA21	1	78.8	0.60	0.13	
PVA22	2	78.3	0.60	0.21	
PVA23	3	77.6	0.59	0.25	Differential pressure (P4) indicates void fraction of 0.25.
PVA24	4	77.2	0.59	0.2	Sump overpressure = 7.3 psig.
PVA25	-	77.6	0.59	0.17	Sump overpressure = 7.3 psig.
PVA26	5	77	0.59	0.22	Sump overpressure = 33 psig.
PVA27	6	71.8	0.55	0.26	
PVA28	7	70.5	0.54	0.30	
PVA29	9	50.5	0.39	0.24	Only partial CS flow rate; long-term downcomer void measurement is 0.5; agglomeration of downward flowing air bubbles is observed.
PV210	-	68	0.52	0.30	
PV211	8	64.5	0.49	0.22	
PV212	10	12.5	0.10	0.	No void transported to downcomer.
PV213	11	80.8	0.62	0.32	Sump overpressure = 0.0 psig. Differential pressure (P4) indicates void fraction of 0.3.
PV214	12	78.1	0.60	0.26	MOV stroke time = 10 sec.
PV215	-	63	0.48	0.19	
PV216	-	70.4	0.54	0.21	
PV217	-	77.7	0.60	0.23	
PV218	-	66.7	0.51	0.26	
PV219	-	44.4	0.34	0.17	Agglomeration of downward flowing air bubbles is observed.
PV220	-	66.7	0.51	0.18	
PV221	-	71.5	0.55	0.23	

Test Name	Test Matrix No.	$Q_1 + Q_2 = Q_{TOT}$	Froude Number	Maximum Void Fraction Downcomer	Comments
PV222	-	63	0.48	0.41	Sump overpressure = 7.3 psig.
PV223	-	71	0.54	0.24	HPSI gas separator removed.
PV224	-	77.5	0.59	0.29	HPSI gas separator removed.
PV225	-	75.5	0.58	0.22	HPSI gas separator removed.
PV226	-	65.5	0.50	0.09	HPSI gas separator removed; CS stand pipe and 3″ rings added.
PV227	-	65.5	0.50	0.18	HPSI gas separator removed.
PV228	-	62.5	0.48	0.27	Sump overpressure = 7.3 psig; HPSI gas separator removed.
PV229	-	60.0	0.46	0.61	Sump overpressure = 15.8 psig; HPSI gas separator removed; Sump line initially voided through check valve and elbow at top of downcomer; Differential pressure (P4) indicates void fraction of 0.62.

Figure B-3: Measured void fraction transient in the bottom of the downcomer for test BVA22.

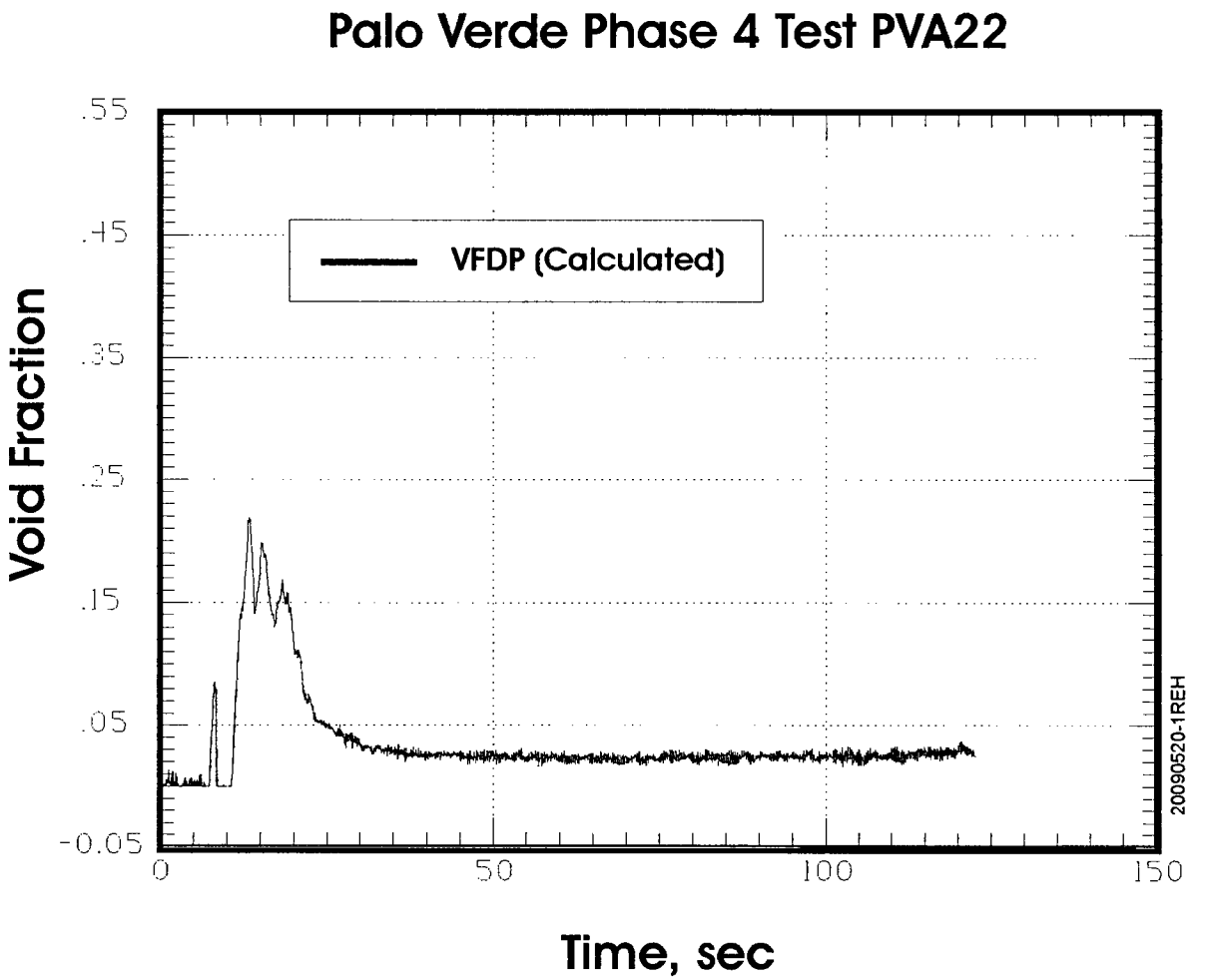

$$W_g = \rho_g \alpha_P A_o (U_o - U_b)$$

where U_b is the bubble rise velocity taken to be 1 ft/sec. The void fraction is the only parameter varying in this equation and the instantaneous mass flow rates are integrated to determine the extent of the gas mass that is observed to exit the bottom of the downcomer.

Figure B-4 illustrates the comparison of the calculated gas mass removed from the bottom of the downcomer compared to the initial gas mass. As noted, this demonstrates that essentially all of the gas is typically removed through the bottom of the downcomer but there is some residual gas that is left in the high point piping. Residual gas volumes were observed in the high point location for several tests.

The experimental data were also evaluated with respect to the measured void fractions in the bottom of the downcomer. For the test conditions of a Froude number of 0.6, the one-dimensional velocity in the 4 inch ID pipe is 2 ft/sec and therefore the velocity in the 3 inch ID downcomer is 3.6 ft/sec. For the tests performed with this Froude number, the kinematic shock was observed to be about 1 foot below the bottom of piping high point, i.e. the additional velocity increase due to gravitational acceleration is about 8 ft/sec. Hence, the kinematic shock involved complete disintegration of the incoming jet such that the void fraction of the flow at that location would be about 0.23. Considering the bubble rise velocity given above, the slip ratio (k_s) 0.72 and the void fraction of the flow being transported to the pump would be approximately 0.29.

Figure B-5 shows that this represents the upper limit of values observed for Froude numbers of 0.6 (velocity of 0.61 m/sec). As the Froude number decreases, the buoyancy influence increases and some large values of local void fraction can occur. Nonetheless, this method of assessing the void fraction at the bottom of the downcomer is demonstrated to be consistent with experiments and if anything conservatively biases to the maximum value.

Figure B-4: Comparison of the gas transport toward the pump compared to the initial gas inventory in the high point.

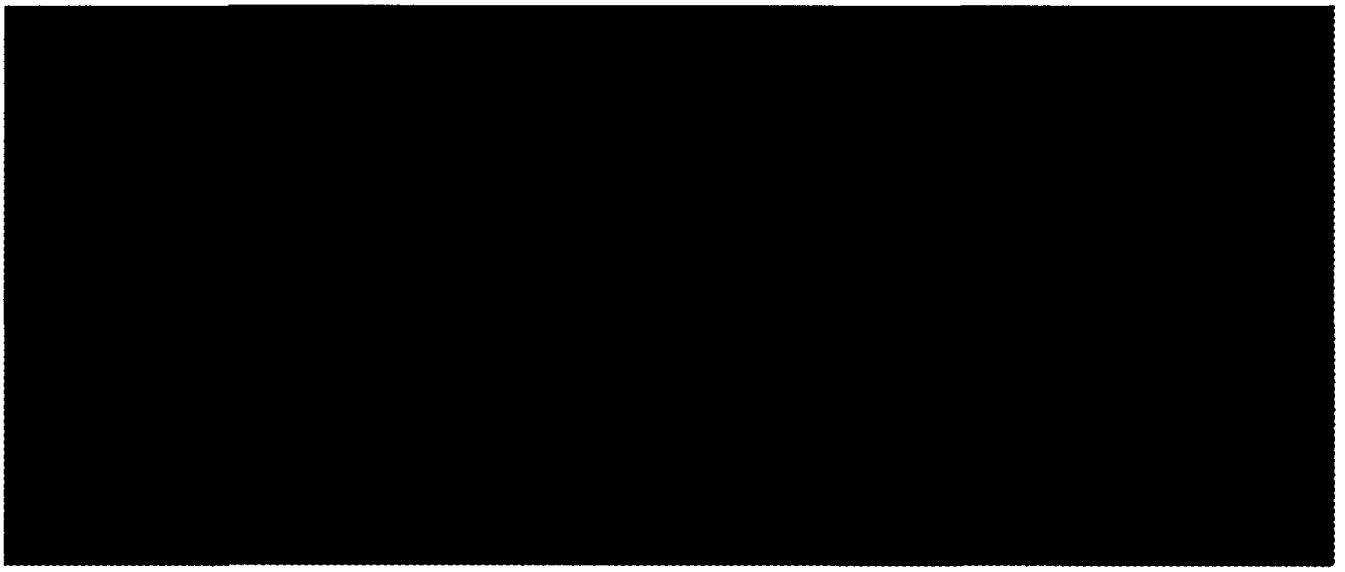

Figure B-5: Measured local void fractions at the bottom of the downcomer for the Palo Verde integral system scaled tests.

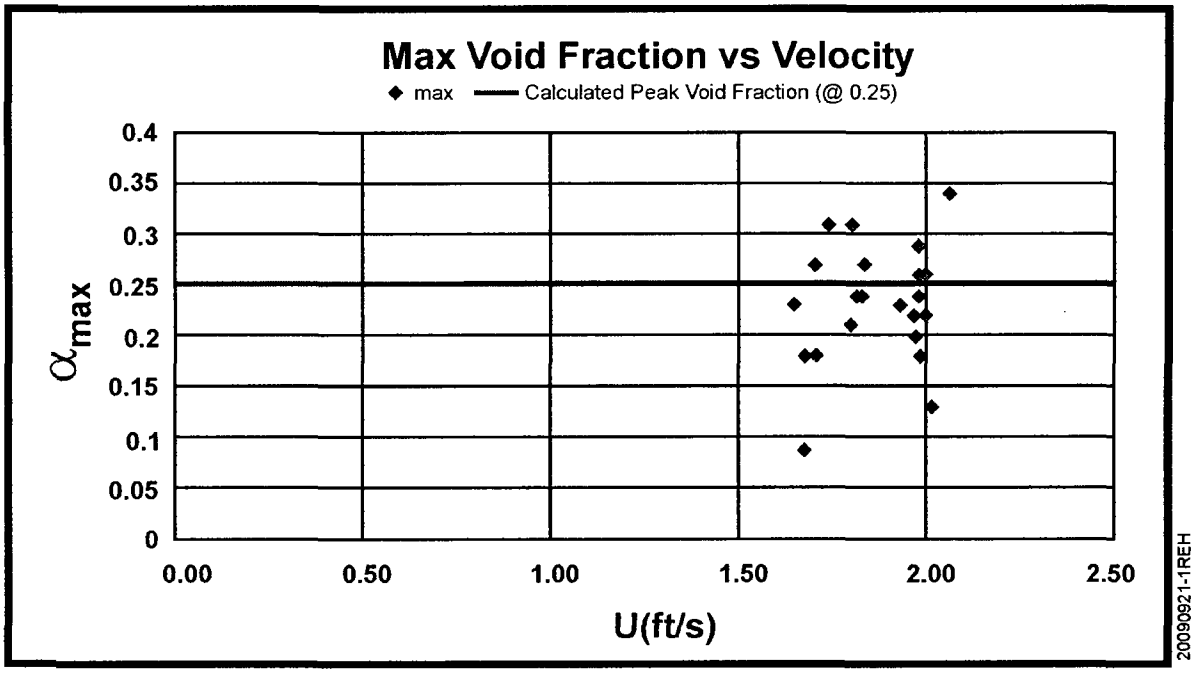

APPENDIX C

Sample Problems

Table C-1

Example #1 of a Possible Plant Condition

D = 24 in (0.6 m) ; L = 50 ft (15.3 m)

A = 3.14 ft^2 (0.292 m^2) $\alpha_o = 0.05$

$V_{go} = 0.05\ (3.14)\ 50 = 7.85\ ft^3$

$N_F = 1.0$ U = 8 ft/sec $Q_w = 25.2\ ft^3/sec = 11{,}310$ gpm

y = 4.20 ft

$$\bar{Q}_g / Q_w = 0.029\left(\frac{y}{D}\right)^{0.68} = 0.048 = \frac{\bar{\alpha}}{1-\bar{\alpha}}$$

$\bar{\alpha} = 0.046$

$$Q_{g,max} / Q_w = 0.049\left(\frac{y}{D}\right)^{0.68} = 0.0811 = \frac{\alpha_m}{1-\alpha_m}$$

$\alpha_m = 0.075$

The average void fraction is slightly less than the initial high point void fraction.

Table C-2

Transition Duration

$$\bar{Q}_g = 0.048\ (25.2) = 1.21\ ft^3/sec$$

$$\Delta t = \frac{V_{go}}{\bar{Q}_g} = \frac{7.85}{1.21} = 6.5\ secs$$

This interval is less than the intervals listed for all pumps in Table 1.

Table C-3

Example #2 of a Possible Plant Condition

$D = 24$ in (0.6 m) ; $L = 30$ ft (9.15 m)

$A = 3.14$ ft^2 (0.292 m^2) $\alpha_o = 0.05$

$V_{go} = 0.05\ (3.14)\ 30 = 4.71$ ft^3

$N_F = 1.0$ $U = 8$ ft/sec $Q_w = 25.2$ ft^3/sec = 11,310 gpm

$y = 2.76$ ft

$$\bar{Q}_g \Big/ Q_w = 0.029 \left(\frac{y}{D}\right)^{0.68} = 0.036 = \frac{\bar{\alpha}}{1-\bar{\alpha}}$$

$\bar{\alpha} = 0.035$

$$Q_{g,max} \Big/ Q_w = 0.049 \left(\frac{y}{D}\right)^{0.68} = 0.06081 = \frac{\alpha_m}{1-\alpha_m}$$

$\alpha_m = 0.057$

The average void fraction is slightly less than the initial high point void fraction.

Table C-4

Transition Duration

$$\bar{Q}_g = 0.036\ (25.2) = 0.907\ \text{ft}^3/\text{sec}$$

$$\Delta t = \frac{V_{go}}{\bar{Q}_g} = \frac{4.71}{0.907} = 5.2 \text{ secs}$$

This duration is less than any of the pump acceptance criteria in Table 1.

Table C-5

Example #3 of a Possible Plant Condition

D = 24 in (0.6 m) ; L = 50 ft (15.3 m)

A = 3.14 ft^2 (0.292 m^2) $\alpha_o = 0.15$

$V_{go} = 0.15\ (3.14)\ 50 = 23.6\ ft^3$

$N_F = 1$ U = 8 ft/sec $Q_w = 25.2\ ft^3/sec = 11{,}310$ gpm

y = 10.7 ft

$$\bar{Q}_g \Big/ Q_w = 0.029\left(\frac{y}{D}\right)^{0.68} = 0.0907 = \frac{\bar{\alpha}}{1-\bar{\alpha}}$$

$\bar{\alpha} = 0.083$

$$Q_{g,max} \Big/ Q_w = 0.049\left(\frac{y}{D}\right)^{0.68} = 0.153 = \frac{\alpha_m}{1-\alpha_m}$$

$\alpha_m = 0.13$

The average void fraction is less than the initial void fraction in the high point.

Table C-6

Transition Duration

$$\bar{Q}_g = 0.0907\ (25.2) = 2.29\ ft^3/sec$$

$$\Delta t = \frac{V_{go}}{\bar{Q}_g} = \frac{23.6}{2.29} = 10.3\ secs$$

Depending on the pump, this may be within the acceptance criterion or longer than the allowable limit.

Table C-7

Example #4 of a Possible Plant Condition

D = 24 in (0.6 m) ; L = 50 ft (15.3 m)

A = 3.14 ft^2 (0.292 m^2) $\alpha_o = 0.10$

$V_{go} = 0.1\ (3.14)\ 50 = 15.7\ ft^3$

$N_F = 1.0$ U = 8 ft/sec $Q_w = 25.2\ ft^3/sec = 11{,}315$ gpm

y = 7.56 ft

$$\bar{Q}_g \Big/ Q_w = 0.029\left(\frac{y}{D}\right)^{0.68} = 0.0716 = \frac{\bar{\alpha}}{1-\bar{\alpha}}$$

$\bar{\alpha} = 0.067$

$$Q_{g,max} \Big/ Q_w = 0.049\left(\frac{y}{D}\right)^{0.68} = 0.121 = \frac{\alpha_m}{1-\alpha_m}$$

$\alpha_m = 0.11$

The average void fraction is somewhat less than the initial high point void fraction.

Table C-8

Transition Duration

$$\bar{Q}_g = 0.0716\ (25.2) = 1.80\ ft^3/sec$$

$$\Delta t = \frac{V_{go}}{\bar{Q}_g} = \frac{15.7}{1.80} = 8.7\ secs$$

The interval is greater than the acceptance criteria for some pumps and shorter than others.

APPENDIX D

Resolution of NRC Comments

The original version of this report was submitted to the NRC to provide comments on the structure of the evaluations and the manner in which this is to be used in plant evaluations. The general questions received are listed in Table D-1 along with the answers to each question. Not surprisingly, the response to these questions adds to the technical basis for the assessing the transmission of a gas volume through more complicated geometries. In particular, the comparison of the information in this report with these somewhat more complicated geometries demonstrates the conservatism embedded in using the downcomer criterion: i.e. the piping high point gas volume in should not be greater than $1/4^{th}$ of the volume in the longest downcomer segment (corrected for the influence of the static head) between the high point and the pump.

Table D-1

Questions on the FAI Report

Question No.	Question	Answer
1	Table 1 comes from the June 18, 2009 NEI letter. Aspects of this table are not consistent with what was agreed to during the 2010 meeting. Differences include statements about disallowing slug flow versus an expectation of peak void being less than 1.7 times the average void.	Table 1 will be updated to be consistent with the current agreed to format and values.
2	Page 27 - Don't the flow conditions at the entrance from the vertical to the lower horizontal violate the homogeneous flow assumption? Does it apply here?	The transition from the vertical downcomer to a horizontal pipe certainly generates flow patterns that are not homogeneous in character. Specifically, conditions are observed with gas tending to move back up the downcomer. These behaviors would act to "stretch-out" the gas void being transmitted toward the pump and therefore reduce the average void fraction being ingested by the pump during the two-phase flow transient. Therefore, it is conservative to evaluate the gas transport as a homogeneous mixture because it maximizes

		the gas transport rate to the pump(s). The answer to the second question is that the homogeneous is applicable here as a conservative assumption that maximizes the calculated rate of gas transport to the pump.
3	Is the Froude number of 0.5 too small to allow the homogeneous flow assumption to apply?	At this low Froude number, the gas would be transported out of the high point location much slower than is calculated using the homogeneous assumption. Therefore, the use of a homogeneous assumption is also a conservative representation of the gas transport to the pump suction port(s) for lower Froude number flows.
4	What is the maximum void fraction in a horizontal section where the methodology applies?	The kinematic shock model represents the maximum and average void fractions that would be generated as the separated two-phase mixture transitions to bubbly flow in the downcomer. As the bubbly mixture flows into a horizontal pipe at the bottom of the downcomer, buoyancy forces can cause gas bubbles to rise and recirculate in the elbow to the horizontal duct. (The lower the Froude number, the more important these buoyancy forces become in recirculating the mixture.) Any such action will tend to "stretch-out" the gas transport and reduce the average void fraction that reaches the pump suction location. Hence, as noted above, the homogeneous model is a conservative representation for the rate of gas transport to the pump.

Gas Void Transmission in More Complicated Configurations

Two important experiments that demonstrate the response of two-phase mixtures, (specifically the flow pattern) to the more complicated piping configurations, are those performed for the HPI suction piping used in Beaver Valley Units 1 and 2. There are significant differences in the HPI suction piping for Units 1 and 2, hence, separate test configurations were used. Both of these scaled experiments were performed in the FAI laboratories (FAI, 1997a and FAI, 1997b).

a, c

Figure D-1: Schematic illustration of the scaled experimental configuration used for the Beaver Valley Unit 1 suction piping for the HPI pumps.

a, c

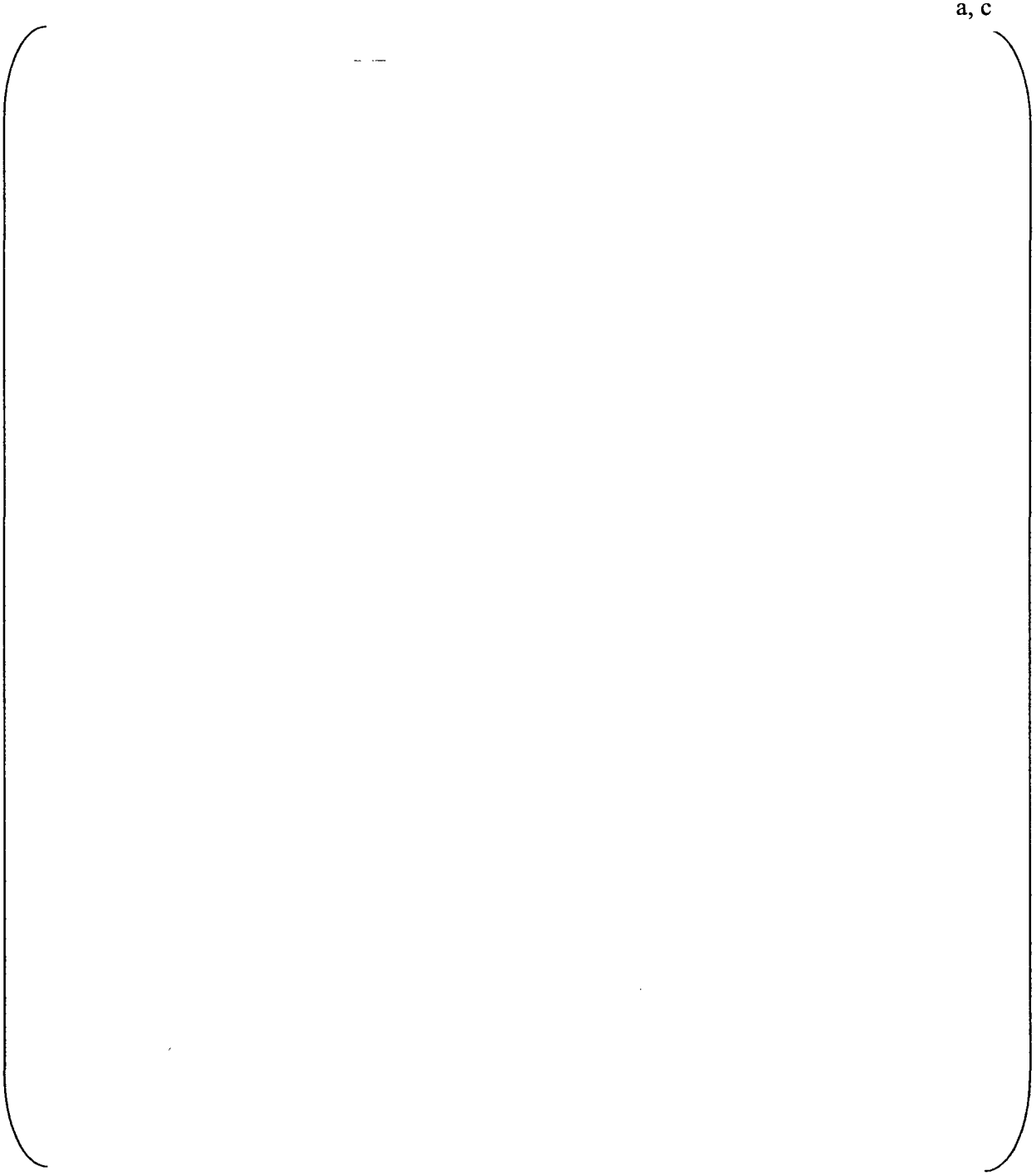

Figure D-2: Comparison of the kinematic shock model and the simplified equation with the measured void fractions in the upper downcomer as a function of the initial void fraction in the high point header.

a, c

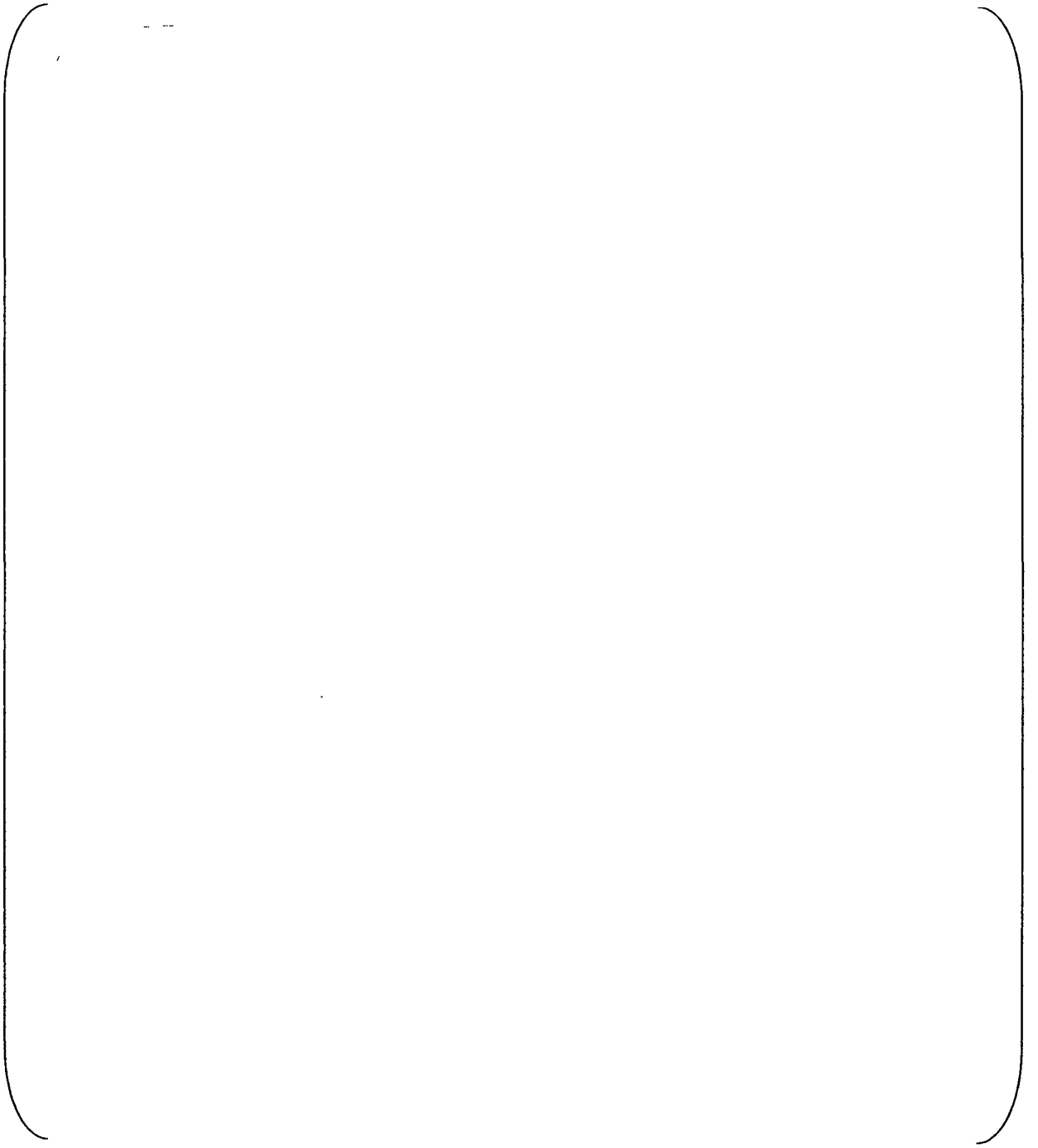

a, c

Figure D-3: Comparison of the kinematic shock model and the simplified equation with the measured void fractions in the lower downcomer as a function of the initial void fraction in the high point header.

a, c

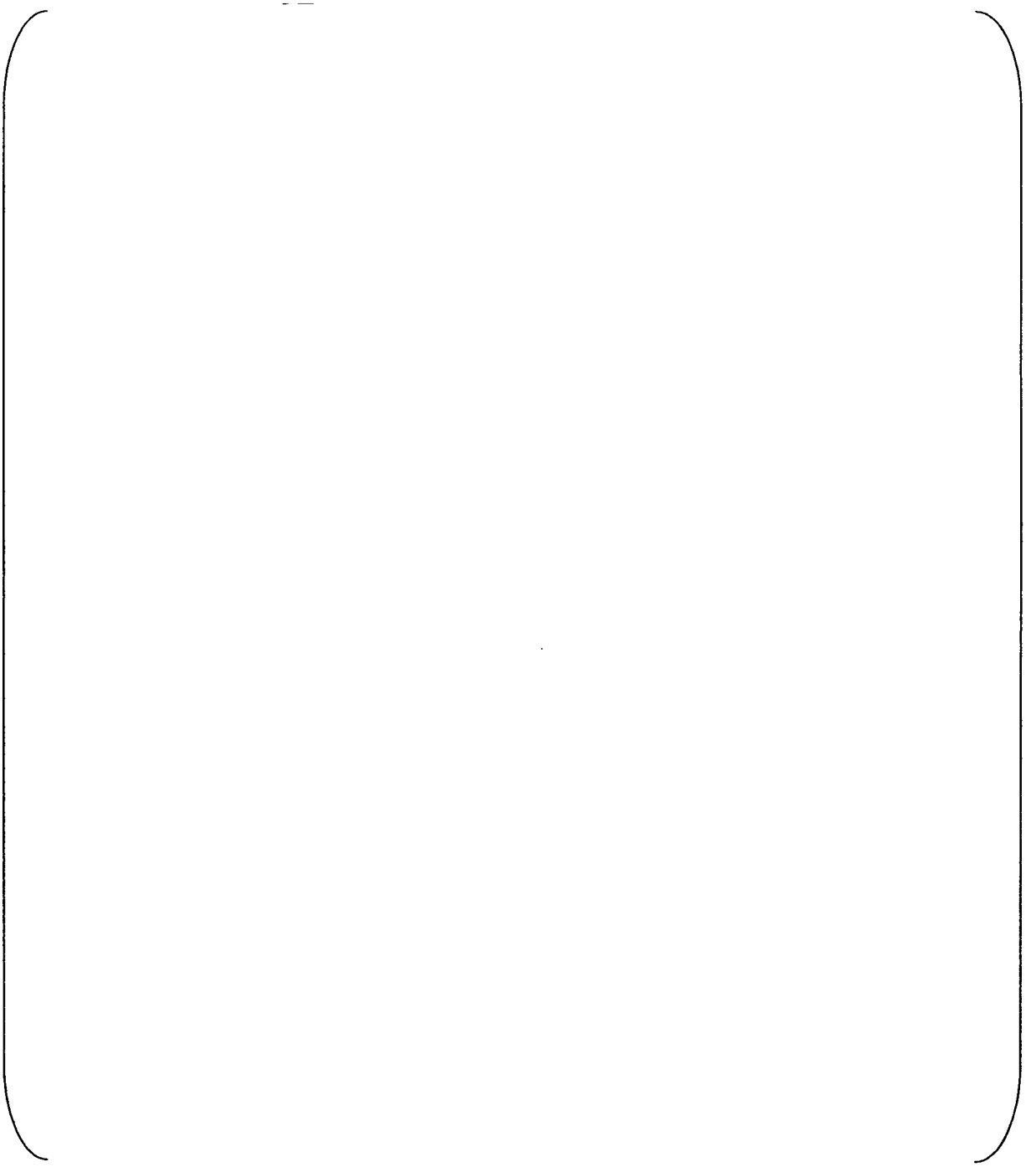

Figure D-4: Schematic illustration of the scaled experimental configuration used for the Beaver Valley Unit 2 suction piping for the HPI pumps.

a, c

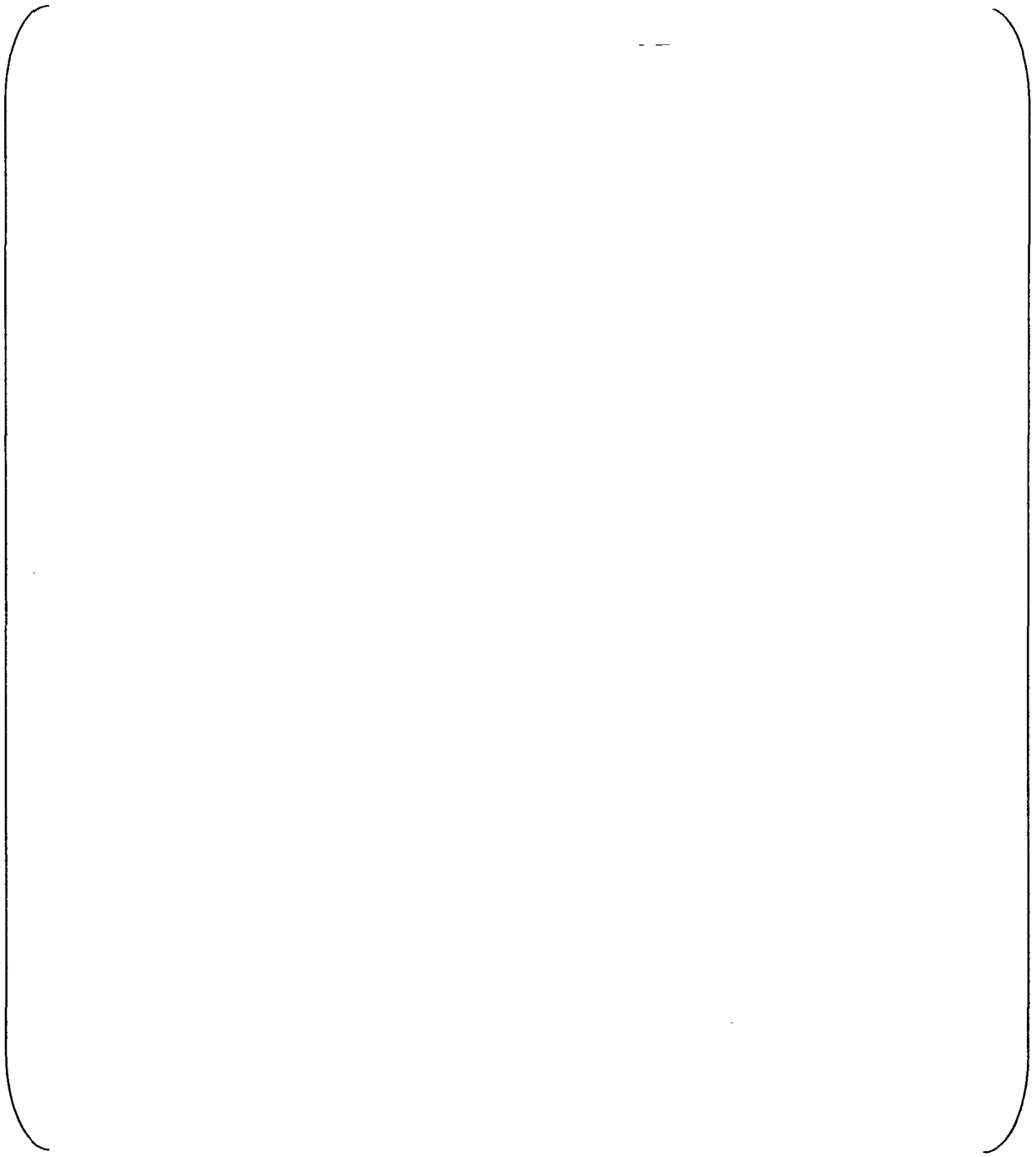

Figure D-5: Comparison of the kinematic shock model with the measured void fractions in the top of the downcomer for the Unit 2 suction piping as a function of the initial void fraction in the high point header.

a, c

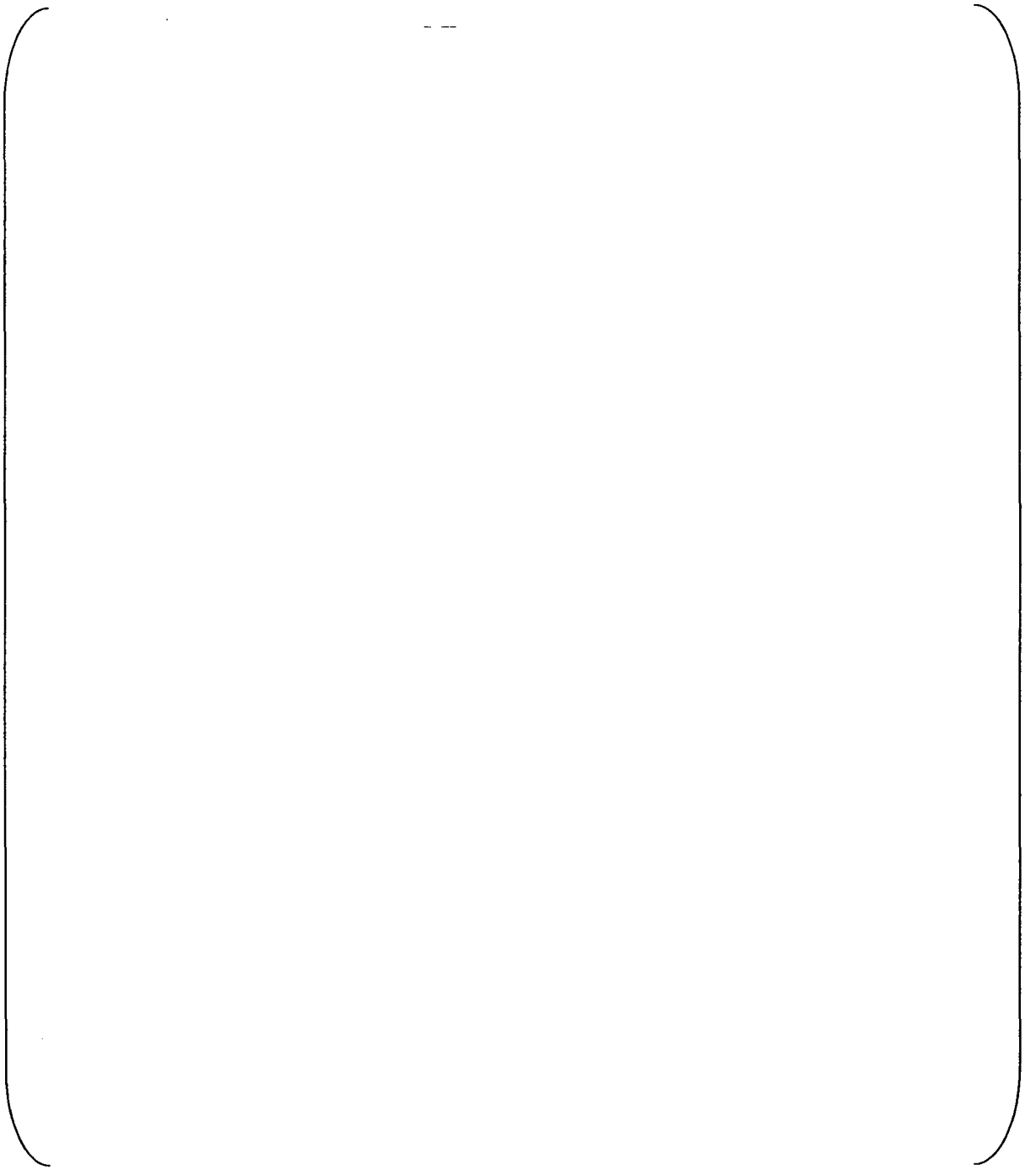

a, c

In summary, these experiments with more complicated suction show that the kinematic shock model is in good agreement with the measured data for the maximum developed at the bottom of the downcomers for the two Beaver Valley units. Moreover, the criterion for ensuring that gas slugs are broken-up by the kinematic shock in the downcomer provides a conservative representation of the kinematic shock capabilities to develop the desired bubbly flow pattern.

References

Fauske and Associates (FAI), 1997a, "Scoping Experiments to Assess the Two-Phase Flow Patterns Entering the Beaver Valley Unit 2 Charging Pumps", FAI/97-125.

Fauske and Associates (FAI), 1997b, "Scoping Experiments to Assess the Two-Phase Flow Patterns Entering the Beaver Valley Unit 1 Charging Pumps", FAI/97-134.

Figure D-6: Comparison of the kinematic shock model and the simplified equation with the measured void fractions in the bottom of the downcomer for the Unit 2 suction piping as a function of the initial void fraction in the high point header.

a, c

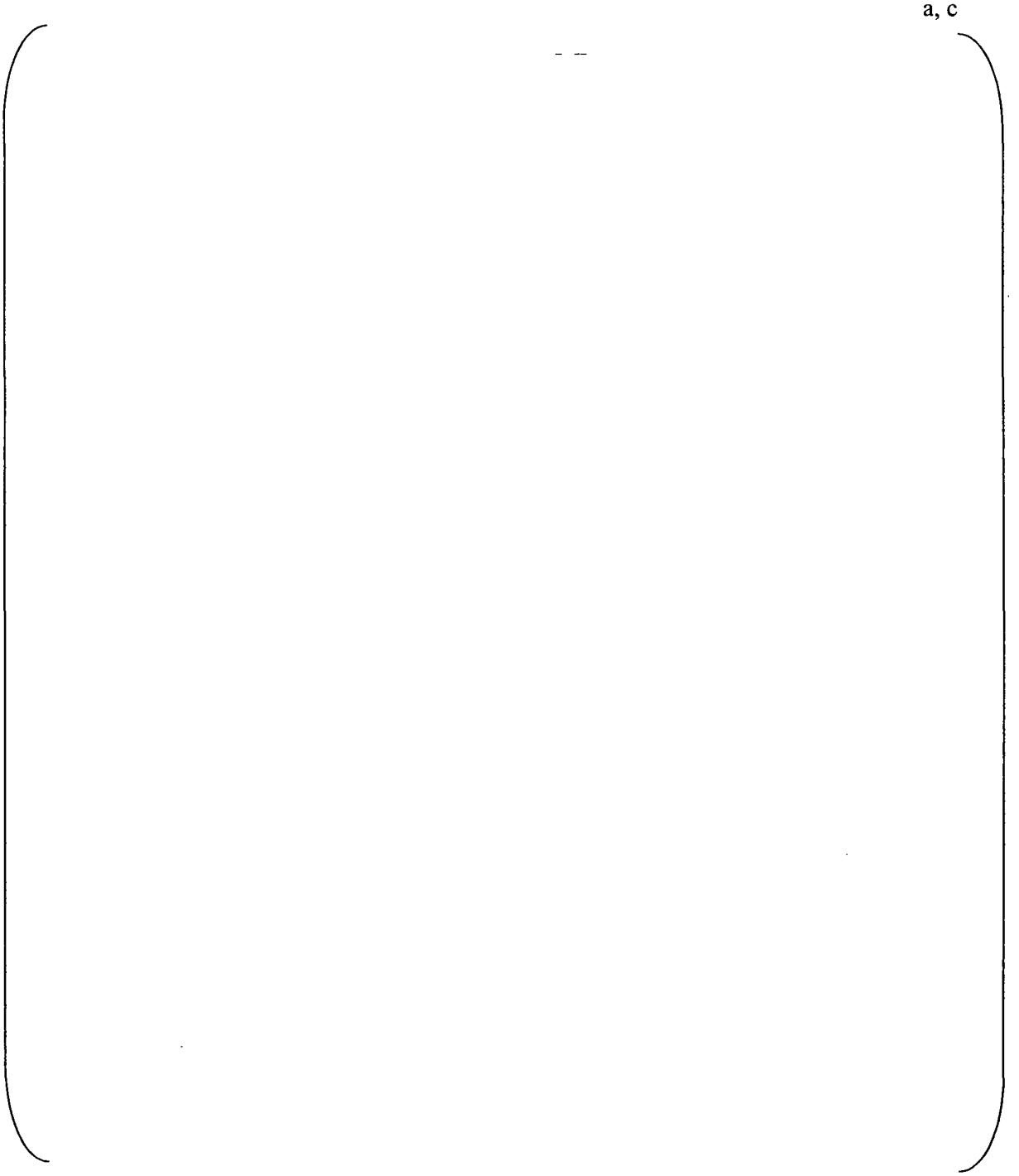

Table D-2

a, c

[ ]